Modélisation des transitions de phases en champ de phase cristallin

Helena Zapolsky

GPM, UMR 6634

GROUPE DE PHYSIQUE DES MATERAUX
Université de Rouen

GDR ModMat, Marseille 21-22 février 2013

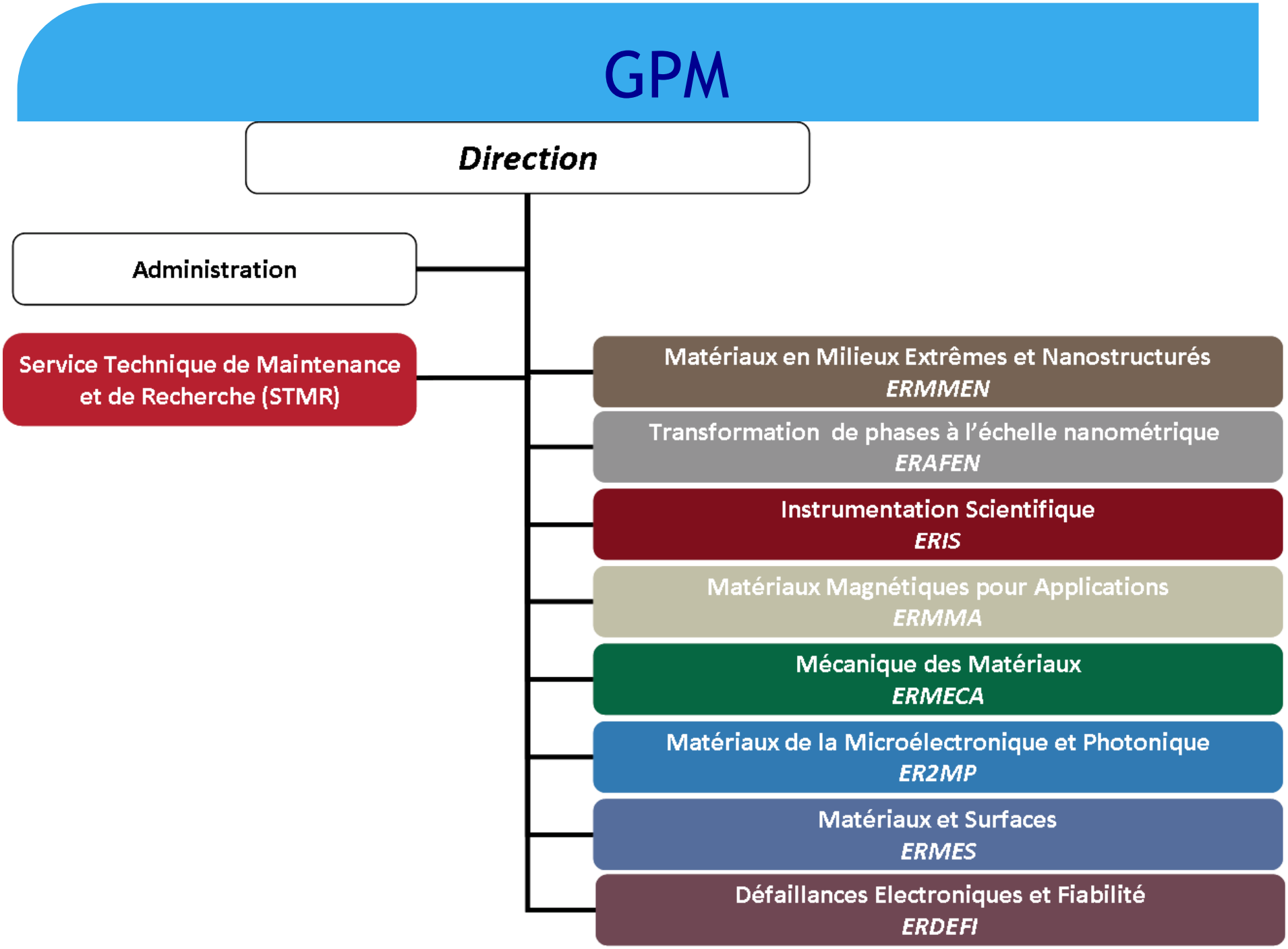
GPM
Direction
Administration
Service Technique de Maintenance et de Recherche (STMR)
Matériaux en Milieux Extrêmes et Nanostructurés
ERMMEN
Transformation de phases à l'échelle nanométrique
ERAFEN
Instrumentation Scientifique
ERIS
Matériaux Magnétiques pour Applications
ERMMA
Mécanique des Matériaux
ERMECA
Matériaux de la Microélectronique et Photonique
ER2MP
Matériaux et Surfaces
ERMES
Défaillances Electroniques et Fiabilité
ERDEFI

Groupe de Physique des Matériaux

Université et INSA de Rouen, UMR CNRS 6634

Instrumentation
Interaction laser - atom

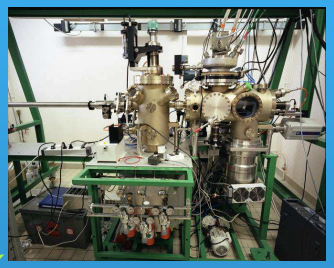

Analyses
Physical metallurgy
and nanomaterials

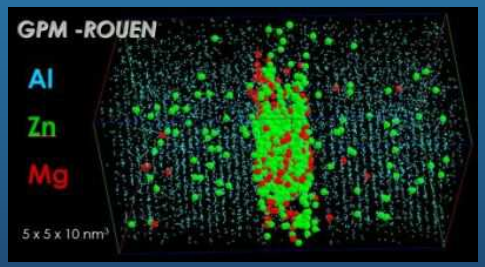

Modeling

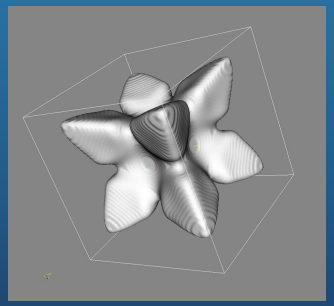

MULTI-SCALE MODELING OF MATERIALS

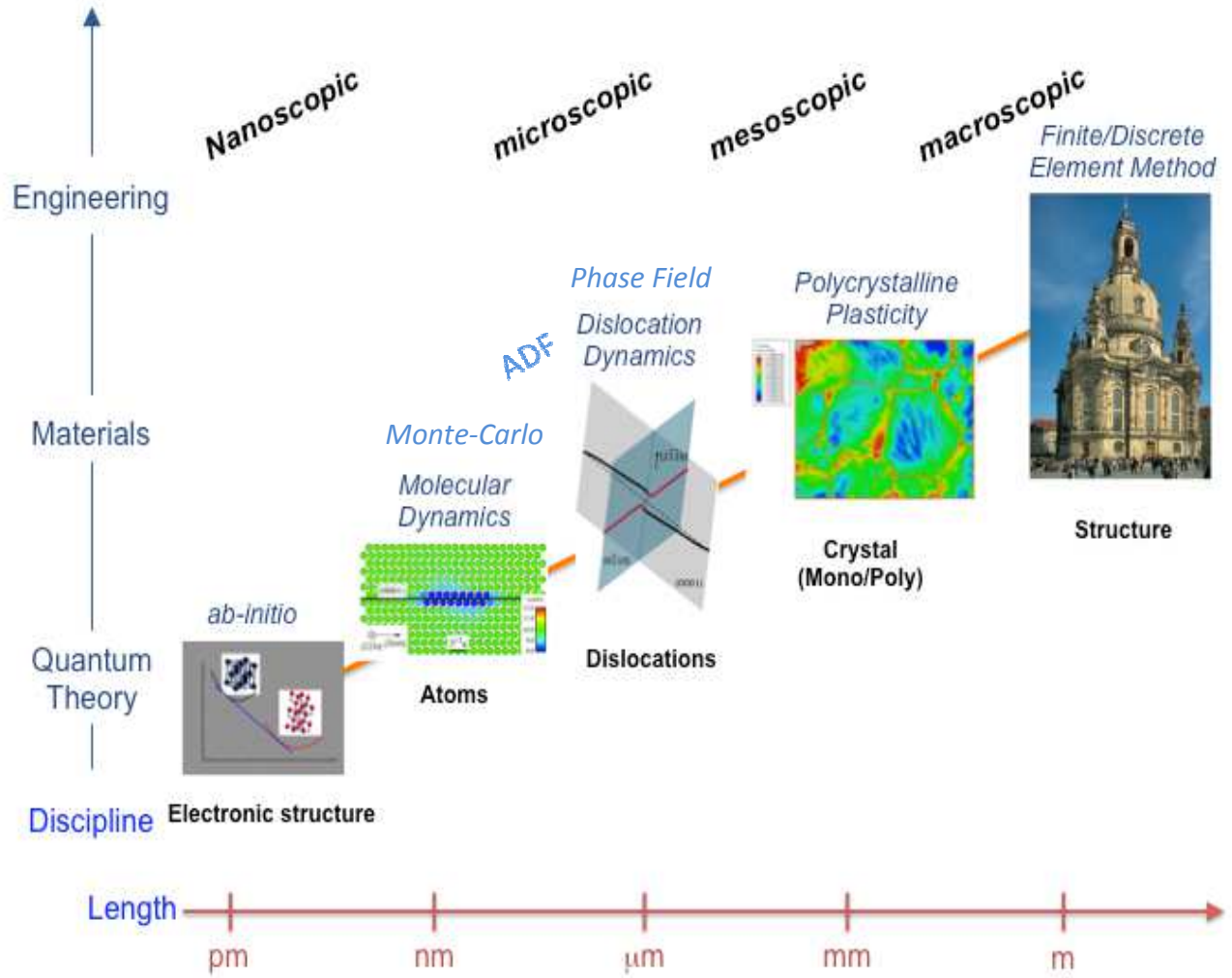

Equation microscopique d'Onsager

Ising lattice Atomic density function (ADF)

$$\frac{dP(r,t)}{dt} = \frac{1}{k_B T} \sum_{\alpha,\beta} \sum_{r'} L_{\alpha\beta}(r-r') c_\alpha c_\beta \frac{\partial F}{\partial P(r',t)}$$

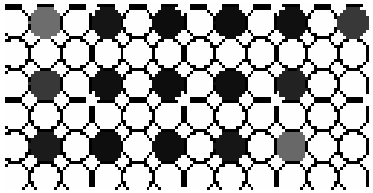

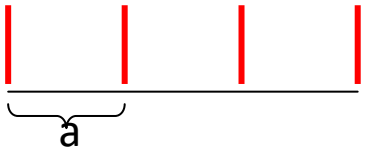

$$F = F_{chem} + E_{elast}$$

Interaction anisotrope à courte portée

Interaction anisotrope à longue portée

Transitions isostructurales

Champ de Phases
Modèle mésoscopique continu

$$\frac{\partial c(\mathbf{r},t)}{\partial t} = \nabla\left(M \nabla \frac{\delta F}{\delta c(\mathbf{r},t)}\right) + \xi_c(\mathbf{r},t)$$

$$\frac{\partial \eta_p(\mathbf{r},t)}{\partial t} = -L \frac{\delta F}{\delta \eta_p(\mathbf{r},t)} + \xi_p(\mathbf{r},t)$$

$$F = F_{chem} + E_{elast}$$

Polynôme de Landau

Interaction anisotrope à longue portée

Echèlle mesoscopique avec interface diffuse

ELASTIC ENERGY

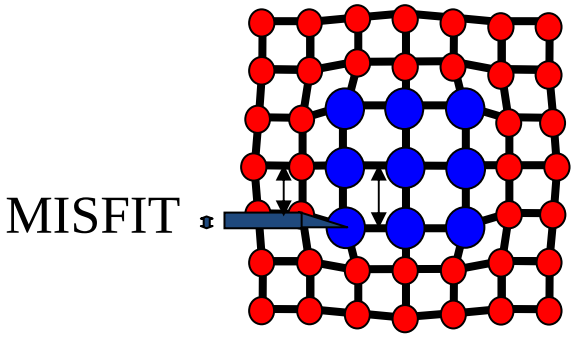

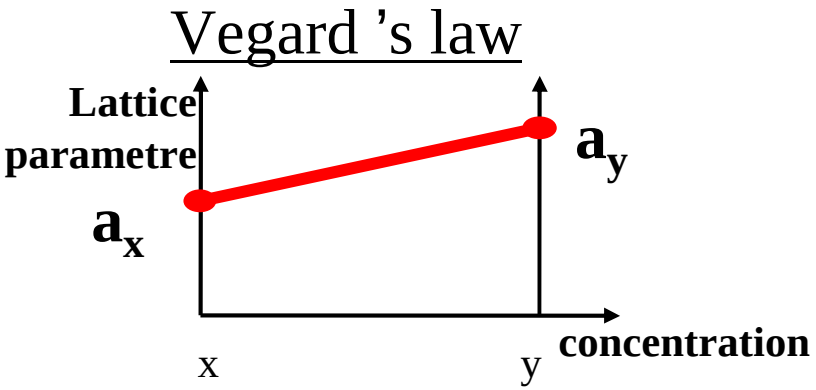

$$E_{elast} = \frac{1}{2}\sum_{pq} \int \frac{d^3k}{(2\pi)^3} B_{pq}(n)\left|\theta(\mathbf{k})\right|^2$$

$$B_{pq}(\mathbf{n}) = c_{ijkl}\varepsilon^0_{ij}(p)\varepsilon^0_{kl}(q) - n_i\sigma^0_{ij}(p)\mathbf{\Omega}_{jk}(\mathbf{n})\sigma_{kl}{}^0(q)n_l$$

Strain-induced interaction between p and q inclusions located at the points R and R '

$$W_{pq}(\mathbf{R}-\mathbf{R}') = -\iiint_{-\infty} \frac{d^3k}{(2\pi)^3}(\mathbf{n}\hat{\sigma}^0(p)\hat{\mathbf{\Omega}}(\mathbf{n})\hat{\sigma}^0(q)\mathbf{n})\left|\theta(\mathbf{k})\right|^2$$

$$\Omega^{-1}_{ij}(\mathbf{n}) = c_{ijkl}n_k n_l$$

$$\mathbf{n} = \frac{\mathbf{k}}{k}$$

ADF sur le réseau d'Ising

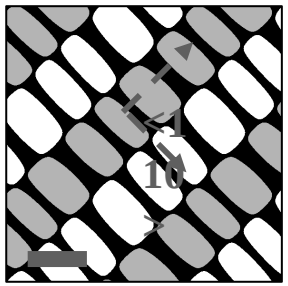

50 nm

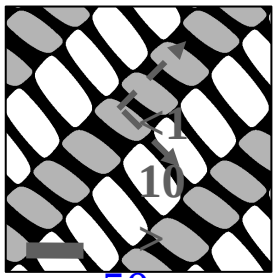

50 nm

d =$\varepsilon_{11}/\varepsilon_{33}$= -0.35

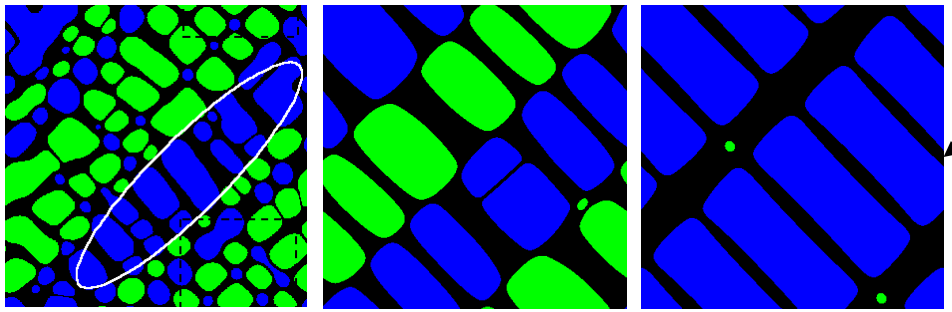

d = -0.5

d=0

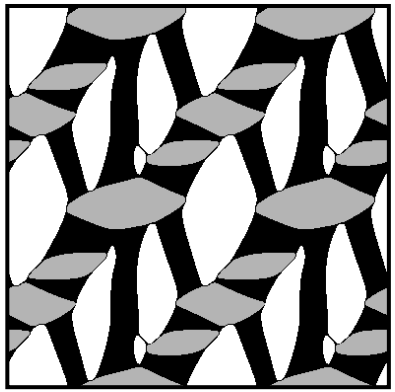

Ni-20V-10Co

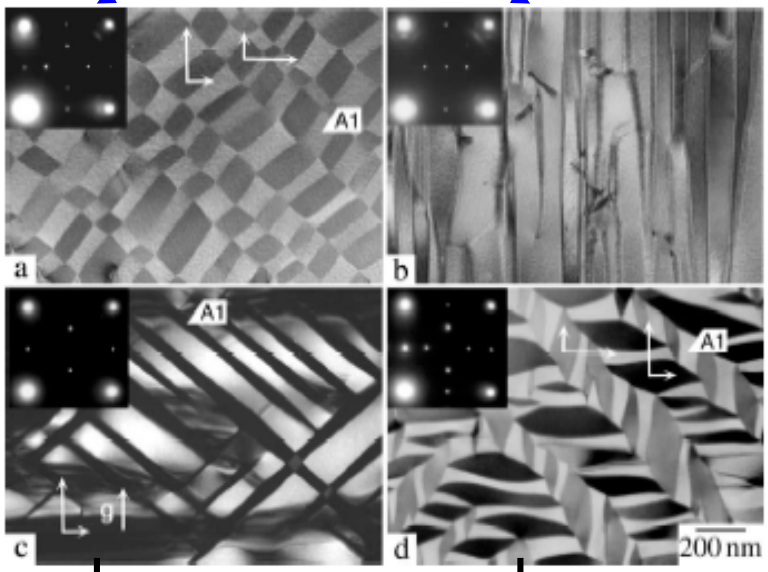

Ni-19V-4Fe

Ni-15V-5Nb

Images de MET des alliages ternaires vieillis à 1073°K 864 ks, A1/DO_{22} microstructure
(A. Suzuki, H. Kojima, T. Matsuo and M. Takeyama, Intermetallics 12 (2004) 969-975)

H. Zapolsky,S. Ferry, X. Sauvage,D. Blavette, L.Q. Chen, Phil. Mag. (2011).
M. Eckholm, H. Zapolsky, A. Ruban, I. Vernyhora, D. Ledue, I. Abrikosov, PRL (2010)

Advanced Microstructure Modeling using Phase Field Method

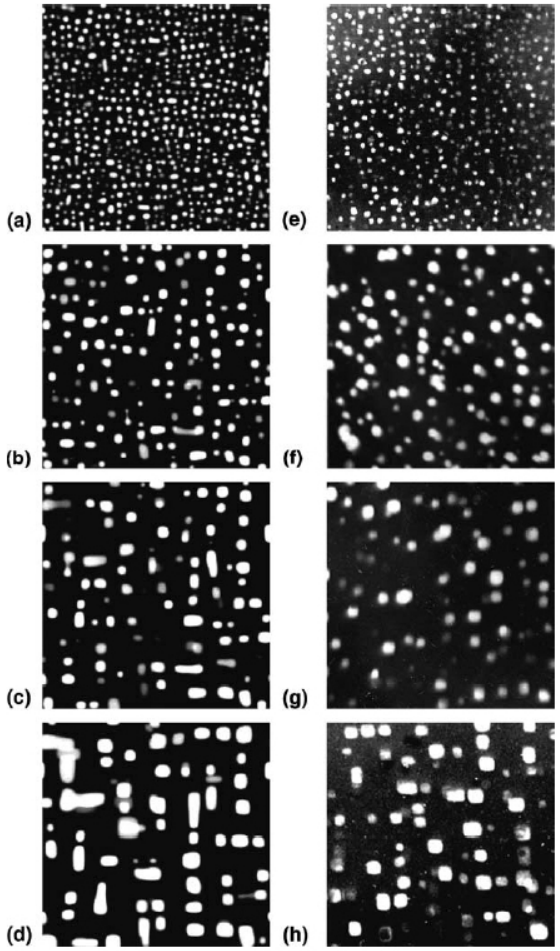

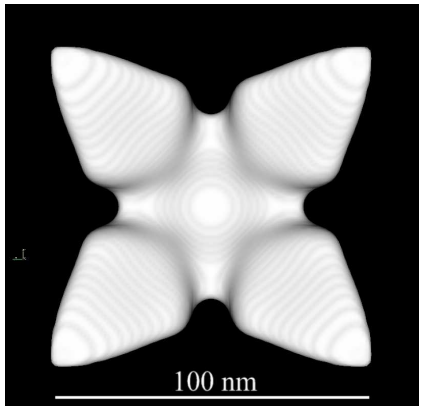

modélisation

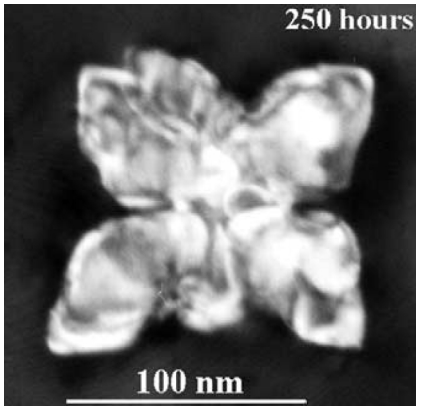

MET

Précipité Al_3Sc en forme de "papillon" observé en MET par Marquis et al. Acta Mat., 49(11) 2001 dans un alliage Al −0.1wt%Sc vieilli à 350C pendant 250 h.

Comparaison de la morphologie des précipités de phase Ni_3Al projetés en 2D (640Å~640 nm), obtenus par simulations en champ de phase (colonne de gauche) et par images MET (colonne de droite) dans un alliage Ni−13.8at.%Al vieillis à 1023 K : (a),(e) t = 15 min ;(b),(f) t = 2 h ; (c),(g) t = 4 h ; (d),(h) t = 8 h.

Energie chimique

ADF sur un réseau d'Ising

$$F = \frac{1}{2}\sum_{r,r'} V(r-r')\,p(r)\,p(r') + k_B T \sum_{\vec{r}} \{p(r)\,Ln(p(r) + [1-p(r)\,]Ln[1-(p(r)]\}$$

Terme non-local (interaction anisotrope)

Terme local

Champ de Phases

$$F_{chim} = \int_V [\frac{1}{2}\alpha(\vec{\nabla}c)^2 + \frac{1}{2}\sum_{\alpha=1}^{\nu}\beta(\vec{\nabla}\eta_\alpha)^2 + f(c, \eta_1, \eta_2, \ldots \eta_\nu)]dV$$

Non-local term
(interfacial energy)

Local term
density of the bulk free energy

$$f(T,c,\eta) = f_{dés} + A(T,c)\,\eta^2 + B(T,c)\eta^3 + C(T,c)\,\eta^4 + \ldots$$

VOLUME 70, NUMBER 10 PHYSICAL REVIEW LETTERS 8 MARCH 1993

Dynamics of Simultaneous Ordering and Phase Separation and Effect of Long-Range Coulomb Interactions

L. Q. Chen
Department of Materials Science and Engineering, Pennsylvania State University, University Park, Pennsylvania 16802

A. G. Khachaturyan
Department of Materials Science and Engineering, P.O. Box 909, Rutgers University, Piscataway, New Jersey 08855-0909
(Received 18 November 1992)

The finite range interaction

$$V(\mathbf{k})_{fi} = 2W_1[\cos 2\pi h + \cos 2\pi l] + 4W_2 \cos 2\pi h \cos 2\pi l + 2W_3[\cos 4\pi h + \cos 4\pi l], \quad (3)$$

The long-range interaction

$$W(\mathbf{r})_{\text{Coul}} = \frac{A}{r}\exp\left(-\frac{r}{r_D}\right),$$

$$\frac{dn(\mathbf{r},t)}{dt} = \sum_{\mathbf{r}'} L(\mathbf{r}-\mathbf{r}')\frac{\delta F}{\delta n(\mathbf{r}',t)},$$

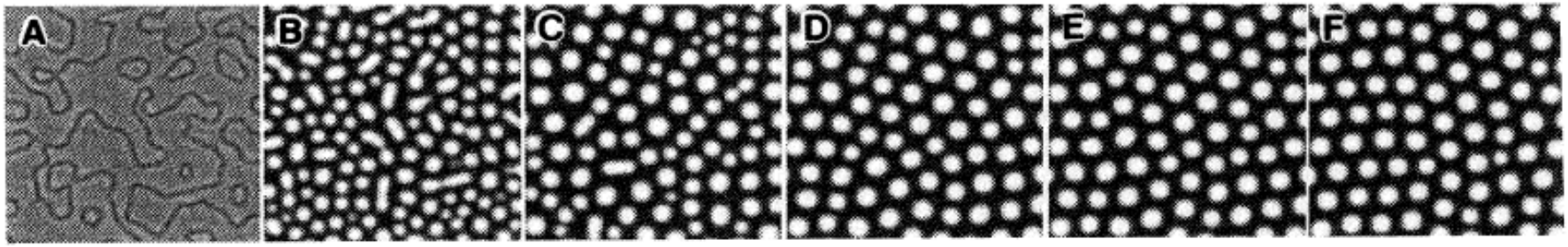

FIG. 2. Temporal morphological evolution started from a completely disordered state with $A=0.25$ eV and composition $c=0.175$. The gray level represents the different magnitudes of the absolute value of $c\eta$, where c is the local composition and η is the local long-range order parameter of the ordered phase; c and η are related to the occupation probability by $n(\mathbf{r})=c(\mathbf{r})+c(\mathbf{r})\eta(\mathbf{r})$. In this representation, bright regions are ordered domains and dark regions are disordered phase domains. (a) $t^*=2.5$; (b) $t^*=10$; (c) $t^*=100$; (d) $t^*=500$; (e) $t^*=1000$; (f) $t^*=2000$.

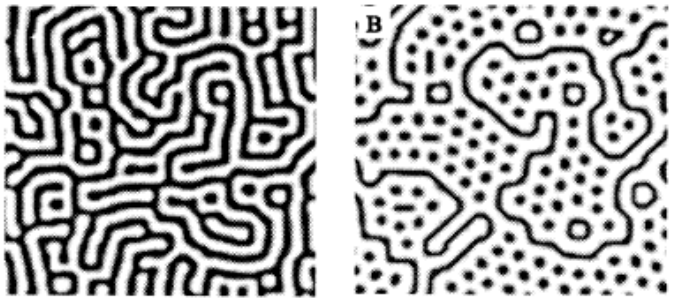

FIG. 5. The influence of average composition on the morphology of the mesoscale phase. The representation is the same as in Fig. 2. (a) $c=0.25$; (b) $c=0.33$. Compare them with Fig. 2(f).

In systems with only finite-range interactions, the resultant two-phase mixture will continuously coarsen reducing its interfacial energy. Our computer simulation demonstrates that the Coulomb interaction stops the coarsening after the ordered particles reach a certain size. Eventually, all ordered particles reach the same size and form a spectacular regular pattern of a triangular lattice [Fig. 2(f)]. Figure 3 shows the corre-

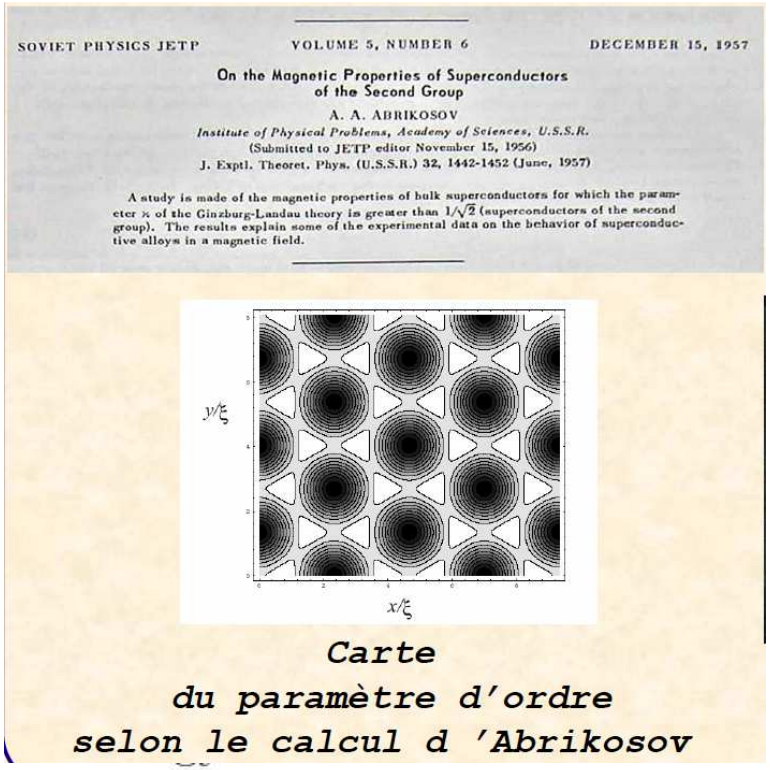

SOVIET PHYSICS JETP VOLUME 5, NUMBER 6 DECEMBER 15, 1957

On the Magnetic Properties of Superconductors of the Second Group

A. A. ABRIKOSOV

Institute of Physical Problems, Academy of Sciences, U.S.S.R.

(Submitted to JETP editor November 15, 1956)

J. Exptl. Theoret. Phys. (U.S.S.R.) 32, 1442-1452 (June, 1957)

A study is made of the magnetic properties of bulk superconductors for which the parameter κ of the Ginzburg-Landau theory is greater than $1/\sqrt{2}$ (superconductors of the second group). The results explain some of the experimental data on the behavior of superconductive alloys in a magnetic field.

Carte du paramètre d'ordre selon le calcul d 'Abrikosov

$|\psi|^2$ proportional to the density of superconducting electrons

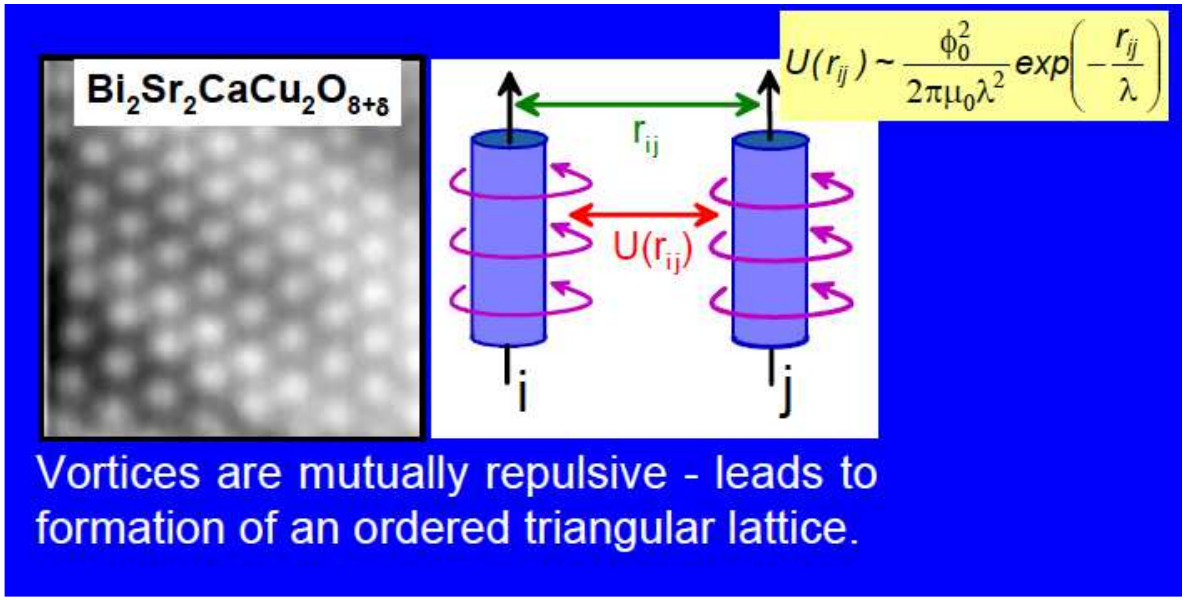

Interaction between the **vortex**:
repulsion -> two wires with currents in opposite directions
attraction->the superconductor prefering to be in a state with no defects.

Turing Patterns in Animal Coats

Reaction–diffusion systems

$$\partial_t u = f(u,v) + D_u \nabla^2 u,$$

$$\partial_t v = g(u,v) + D_v \nabla^2 v.$$

Rayleigh–Bénard convection

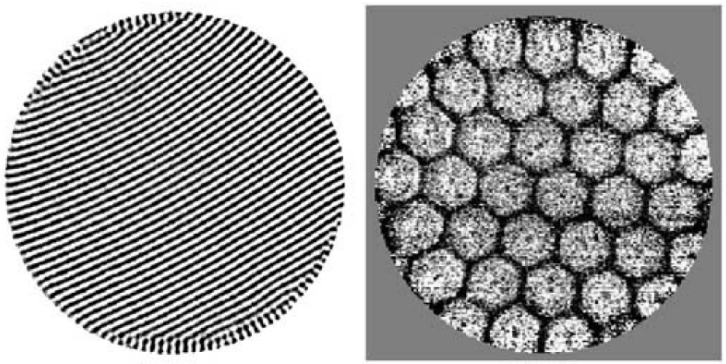

$R=1.2R_c$ $R=1.02R_c$

Swift-Hohenberg model of convection

The "free" energy (Lyapunov function) in SH model is:

$$F=\int d\mathbf{r}\left[\frac{1}{2}\psi(-\varepsilon+(q_0^2+\nabla^2)^2\psi+\frac{\psi^4}{4}\right]$$

The dynamic of ψ is assumed to be dissipative equation:

$$\frac{\partial\psi}{\partial t}=\varepsilon-(q_0^2+\nabla^2)^2\psi$$

Champ de Phase Cristallin

K. R. Elder and M. Grant – Modeling elastic and plastic deformations in nonequilibrium processing using phase field crystals – Phys. Rev. E, Vol. 70, p. 051605 (2004)

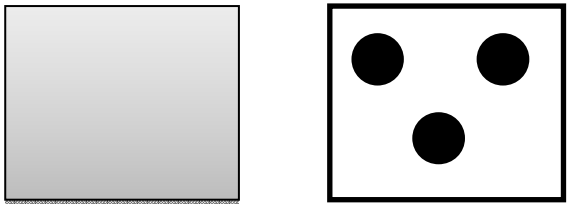

liquide solide

$$F = \int_V \left[-\kappa_1 \left| \vec{\nabla} \psi \right|^2 + \kappa_2 \left| \vec{\nabla}^2 \psi \right|^2 + f(\psi) \right] d^3 r$$

$$\frac{\partial \psi}{\partial \tau} = \vec{\nabla}^2 \left(\frac{\delta F}{\delta \psi} \right)$$

Lien avec DFT

$$\frac{\Delta F[\varphi(\vec{r})]}{k_B T \rho_0} = \int_V [(\varphi(\vec{r})+1)\ln(\varphi(\vec{r})+1) - \varphi(\vec{r})]\, d^3 r - \frac{\rho_0}{2} \int_V \int_V \varphi(\vec{r}) c^{(2)}(\vec{r} - \vec{r}\,') \varphi(\vec{r}\,') d^3 r\, d^3 r$$

$$(1+\varphi)\ln(1+\varphi) - \varphi \approx \frac{1}{2}\varphi^2 - \frac{a}{6}\varphi^3 + \frac{b}{12}\varphi^4$$

$$k_B T \frac{\delta^n F_{xs}}{\delta\rho(\vec{r}_1)..\delta\rho(\vec{r}_n)} = -c^{(n)}(\vec{r}_1,....,\vec{r}_n)$$

$$C(\vec{k}) = C_0 + C_2 \vec{k}^2 + C_4 \vec{k}^4$$

Continuum Atomic Density Function model (Phase Field Crystal)
Y. Jin, A.G. Khachaturyan APL 2006

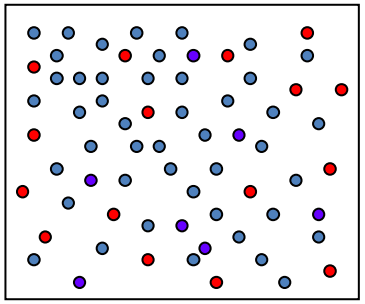

A small parameter determining the transition to microscopique continuum version of ADF model is:

$$\frac{a}{R_{W\alpha\beta}} << 1$$

a- Ising lattice parameter

$R_{W\alpha\beta}$- characteristic distance of interatomic interaction

ADF on constrained lattice

P(r) - probability to find atom at position r

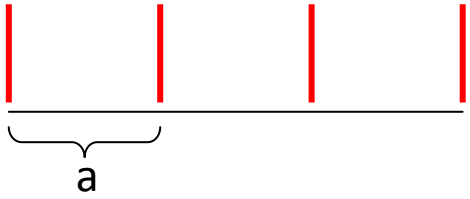

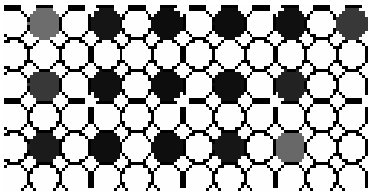

ADF on unconstrained lattice

ρ(r) - atomic density

$$\{\rho(\boldsymbol{r})_\alpha\} = (\rho_1, \rho_2, \ldots, \rho_\alpha, \ldots, \rho_n)$$

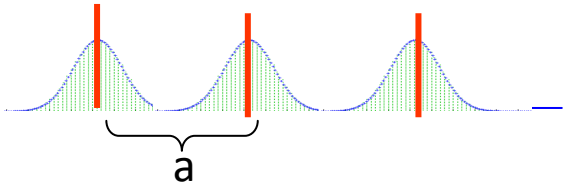

ρ (r) -> averaging over time :

Δ t > frequency of phonons

Δ t < characteristic diffusion time

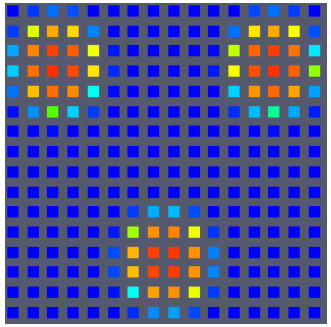

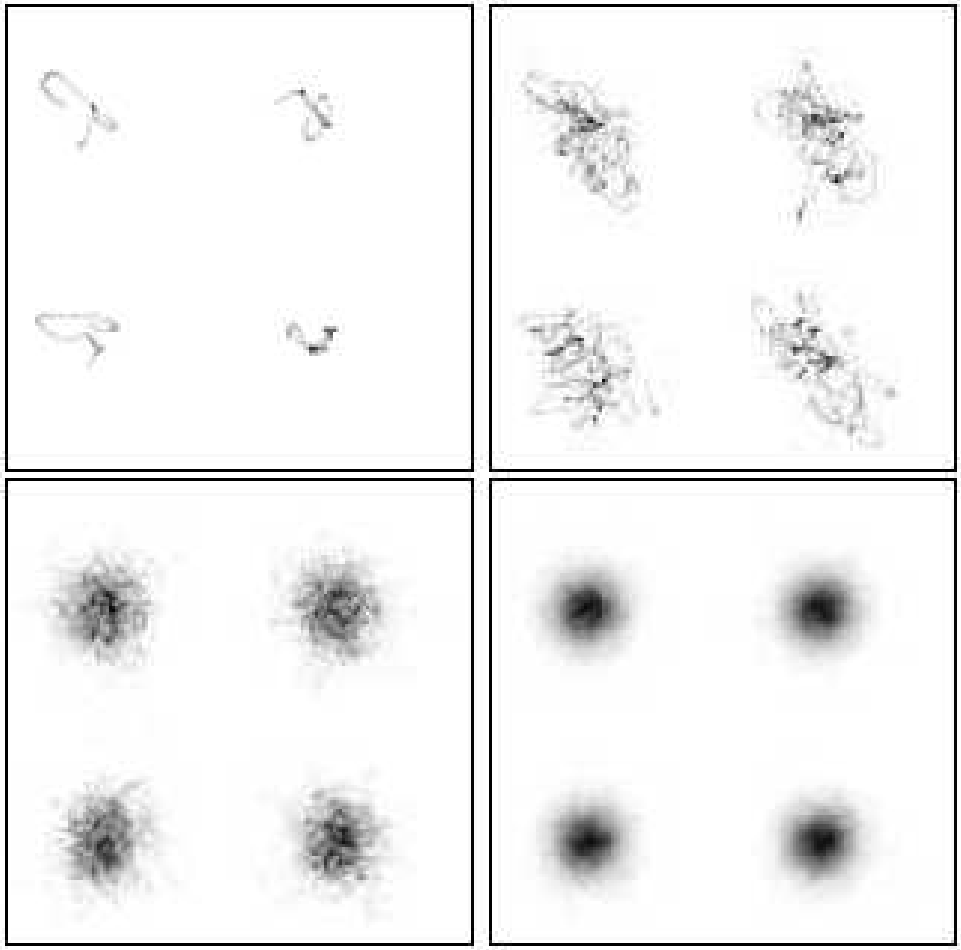

Fig. 1: Grey-scale plot of time-averaged density of portion of Weber–Stillinger MD system for reduced temperature 0.6, reduced density 0.77277. The time intervals for averaging are 1, 10, 100, 1000 time units.

P. F. Tupper and M. Grant – Phase field crystals as a coarse-graining in time of molecular dynamics – Europhys. Lett., Vol. 81, p. 40007 (2008)

Limit transition to the Landau theory

$$F = \int \frac{1}{2}\sum_{\alpha\beta} V_{\alpha\beta}(k)\Phi_{\alpha}(k)\Phi^{*}_{\beta}(k)\frac{d^3k}{(2\pi)^3} + \int_V f(\{\rho_{\alpha}(r)\})d^3r \qquad (1)$$

Where $V_{\alpha\beta}(\mathbf{k})$ is the Fourier transforms of the effective potentials $W_{\alpha\beta}(\mathbf{r})$:

$$\mathrm{V}(\boldsymbol{k}) = \int_{\mathrm{V}} \mathrm{W}(\boldsymbol{r})\exp(-\mathrm{i}\boldsymbol{k}\boldsymbol{r})\mathrm{d}^3\mathrm{r}$$

Using Taylor expansion of $V_{\alpha\beta}(\mathbf{k})$ in k

$$V_{\alpha\beta}(k) = A_0^{\alpha\beta} + \frac{1}{2!}A_2^{\alpha\beta}k^2 + \frac{1}{4!}A_4^{\alpha\beta}k^4 + \ldots + \frac{1}{n!}A_n^{\alpha\beta}$$

Eq.(1) is a generalized **Landau gradient expression**:

$$F = \int_V \sum_{\alpha\beta}\left(\frac{1}{2!}A_o^{\alpha\beta}\rho_{\alpha}(\mathbf{r})\rho_{\beta}(\mathbf{r}) + \frac{1}{2!}A_2^{\alpha\beta}\nabla\rho_{\alpha}(\mathbf{r})\nabla\rho_{\beta}(\mathbf{r}) + \frac{1}{4!}A_4^{\alpha\beta}\nabla^2\rho_{\alpha}(\mathbf{r})\nabla^2\rho_{\beta}(\mathbf{r}) + \ldots\right)d^3r$$
$$+ \int_V f(\{\rho(\mathbf{r})_{\alpha}\})d^3r$$

The **Phase Field Crystal model** (Elder) has used two first terms of the gradient expansion of the Landau theory.

• There is no Ising lattice constraint: atoms are free to continuously move to relax the free energy.

• The n-component system is described by the *n* **atomic density functions**:

$$\{\rho(\boldsymbol{r})_\alpha\} = (\rho_1, \rho_2, \ldots, \rho_\alpha, \ldots, \rho_n)$$

• **The ADF kinetic** equations are essentially the same but the integration is over continuum space is substituted for summation over lattice sites:

$$\frac{\partial \rho_\alpha(\mathbf{r},t)}{\partial t} = \sum_{\beta=1}^{\beta=n} \int_V L_{\alpha\beta}(\mathbf{r},\mathbf{r}') \frac{\delta F}{\delta \rho_\beta(\mathbf{r}',t)} d^3 r' \qquad \alpha = 1, 2, \ldots, n$$

$F(\{\rho_\alpha(\mathbf{r})\})$ is a non-local free energy functional of *n* atomic density functions, $L_{\alpha\beta}(\mathbf{r},\mathbf{r}')$ is the mobility matrix.

The conservation of the number of atoms:

$$\int_V L_{\alpha\beta}(\mathbf{r},\mathbf{r}') d^3 r' = 0.$$

Phase Field Crystal model

Continue model at atomic scale with diffusion time scale

- ***Free energy functional:***

$$f(\{\rho(\mathbf{r})\}) = f_{\text{int.}} + f_{\text{loc.}}$$

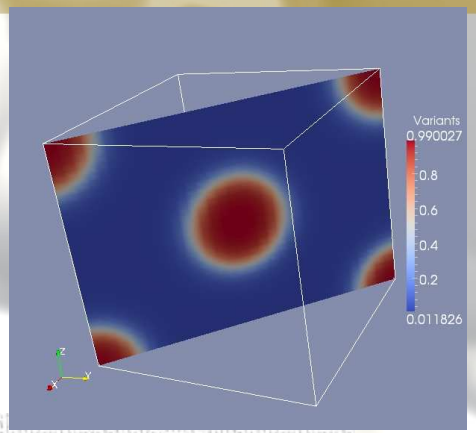

$$f_{\text{int.}} = \int \frac{d^3k}{2\pi} V(k)\rho_{\mathbf{k}}\rho_{-\mathbf{k}}, \quad V(k) = V_0\left(1 - \frac{k^4}{(k^2 - {k_1}^2)^2 + {k_2}^4}\right)$$

- ***Conserved field kinetic equation:***

$$\frac{\partial\rho(\mathbf{r})}{\partial t} = \Gamma\nabla^2\frac{\delta f(\{\rho\})}{\delta\rho(\mathbf{r})}$$

GPM
Groupe de Physique des Matériaux

•Choice of the model parameters for iron

•***Structure factor:***

$$S(k) = k_B T D^{-1}(k)$$

•***Response function:***

$$D(k) = \frac{\delta^2 f(\{\rho\})}{\delta \rho^2} = V_0 \left(1 - \frac{k^4}{(k^2 - {k_1}^2)^2 + {k_2}^4}\right) + \frac{\delta^2 f_{\text{loc.}}}{\delta \rho^2}$$

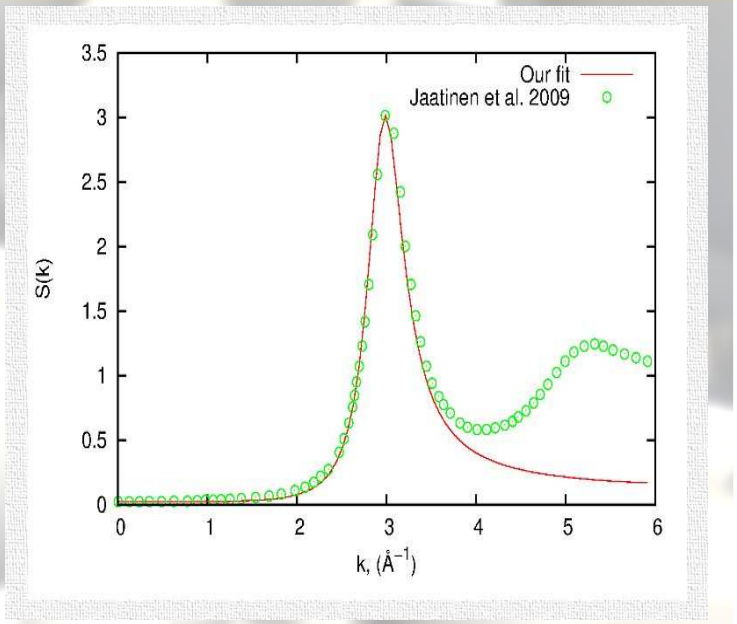

•*Structure factor taken from: Jaatinen et al.s. Rev. E* ***80*** *(2009) 031602*

GPM
Groupe de Physique des Matériaux

• **Paramètres adimensionnés :**

- Simulation en 2 dimensions

- Boîte de simulation : 250 x 250

- Système monoatomique

- = 0.4 $\bar{\rho}$ **L(k) = -k²**

• **Fonction D(k):**

$$D(k,T,\bar{\rho}) = V_0\left[\frac{k^4}{(k^2-k_1^2)^2+\kappa^4}\right] + A_2 + 2A_3\bar{\rho} + 3A_4\bar{\rho}^2.$$

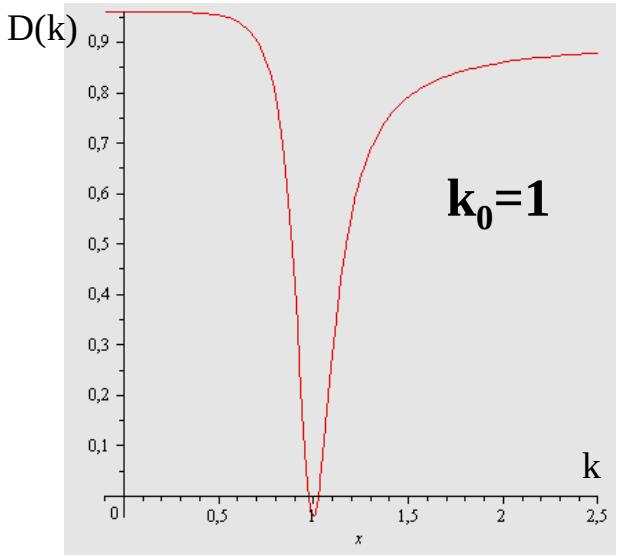

L'état homogène est instable vis-à-vis des fluctuations de longueurs d'onde k_0=1.

La structure stable :

$a_0 \rightarrow \alpha\ k_0$

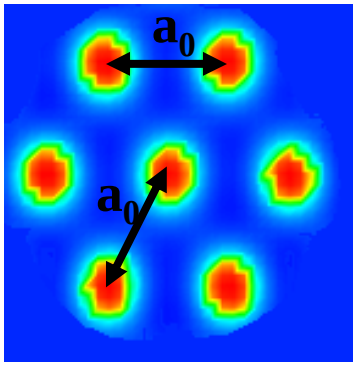

« Liquid – honeycomb » transition

boîte : 256^2
dx = 1.
dt = 0.01

100 000 pas

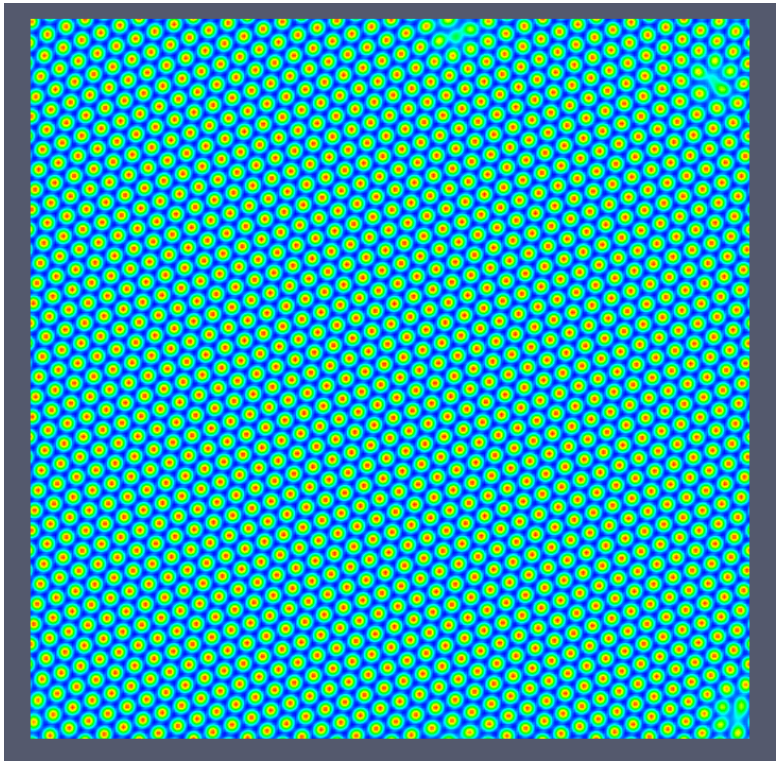

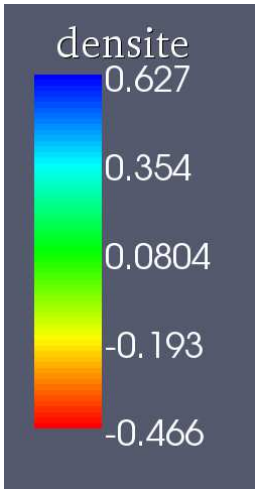

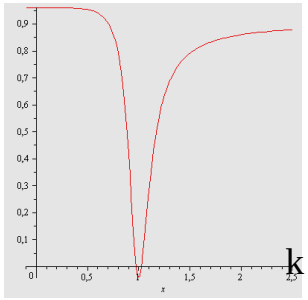

« Liquid – amorphous » transition

- **Function D(k):**

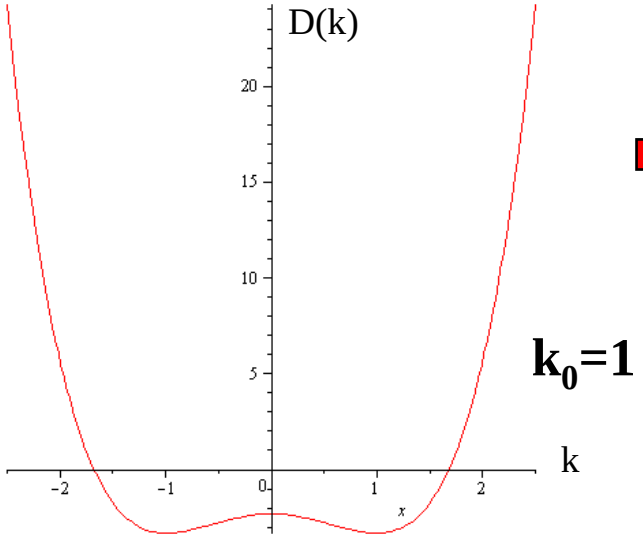

$k_0=1$

The function D(k) becomes negative for a packet of the normal density waves forming a spherical layer in the **k** space around the surface of the radius **k**0 .

$T_c<T<T_0$ the homogeneous metastable liquid state is stable with infinitesimal density modulations

At the deep undercooling **below Tc** , the **continuous wave vector spectrum** of the instability waves formed at the first stage of the transformation **is sufficiently wide**.

Greater is the number of the instability waves formed at the first stage of solidification at **T<Tc** , which have to be eliminated to form the crystal, the **more difficult** is to get rid of the majority of them **to transform the amorphous state to the crystalline one.**

« Liquid – amorphous » transition

Evolution of ρ (r)

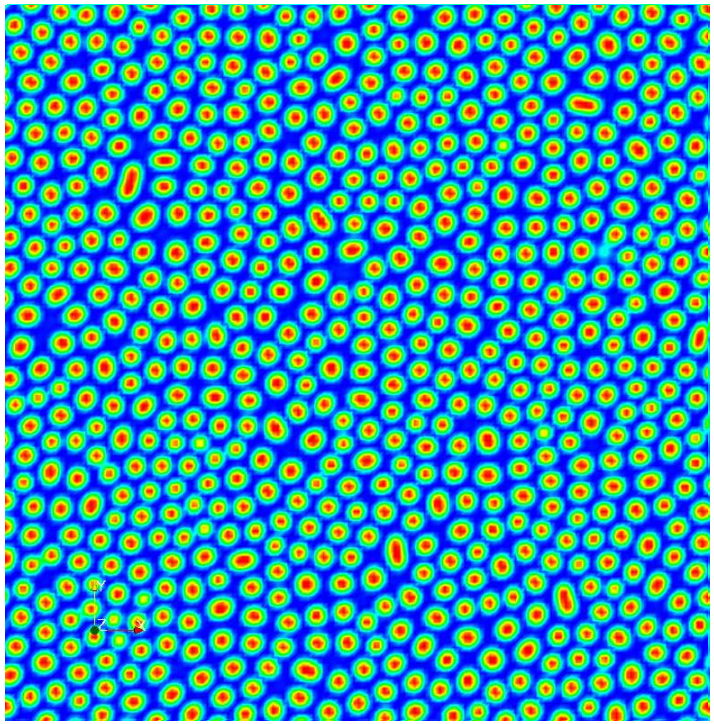

t* = 0.1 → 10

Diffraction pattern

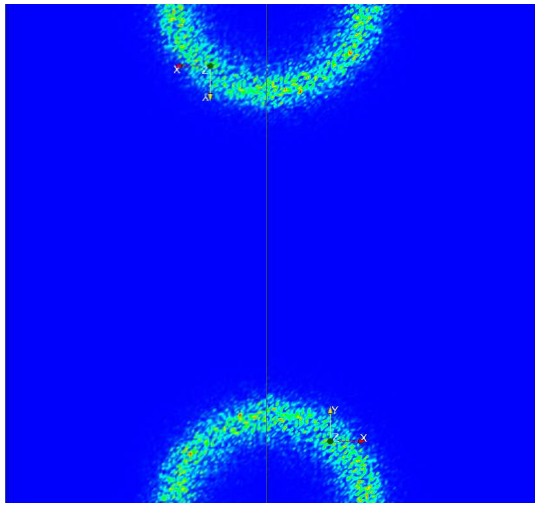

I= ρ (k) ρ *(k)

GB in BCC crystal

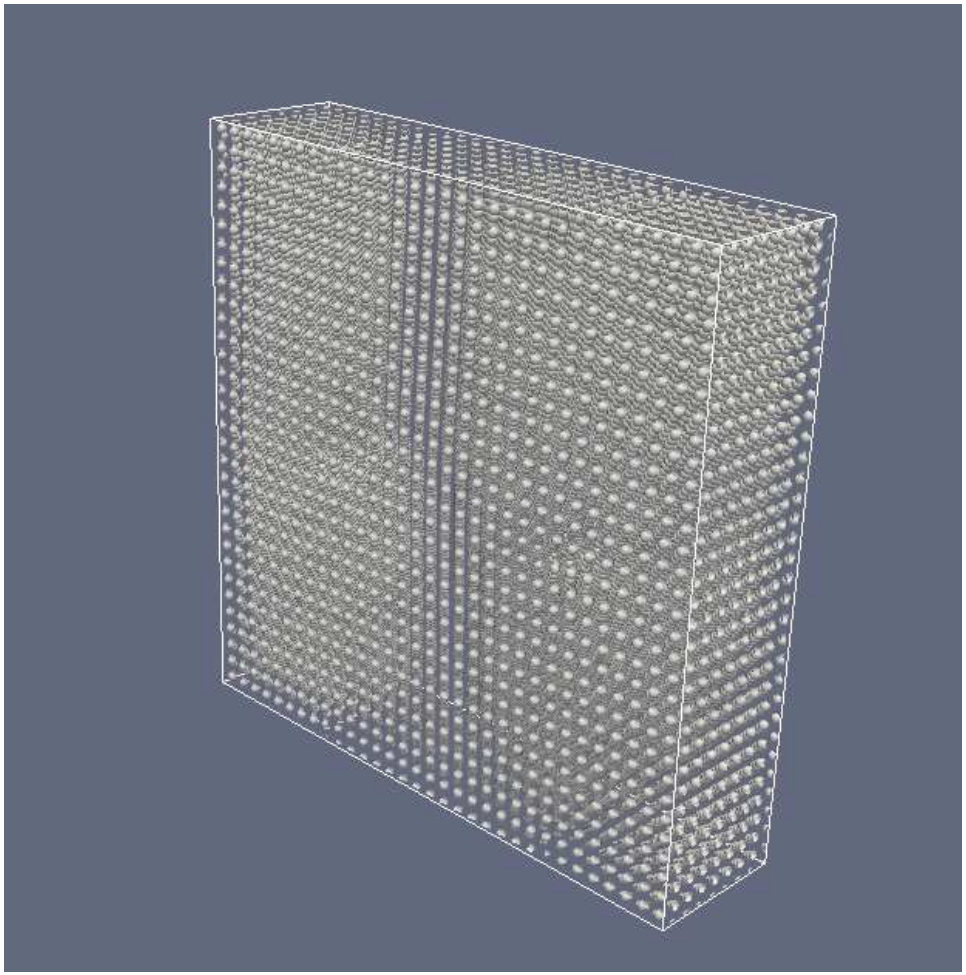

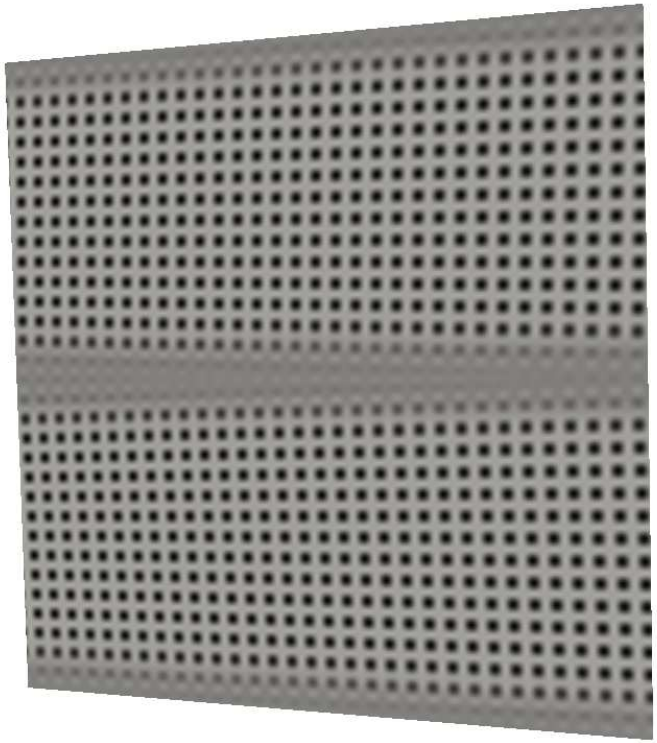

PFC, tilt angle θ = 3.58°

Read and Shockley fit

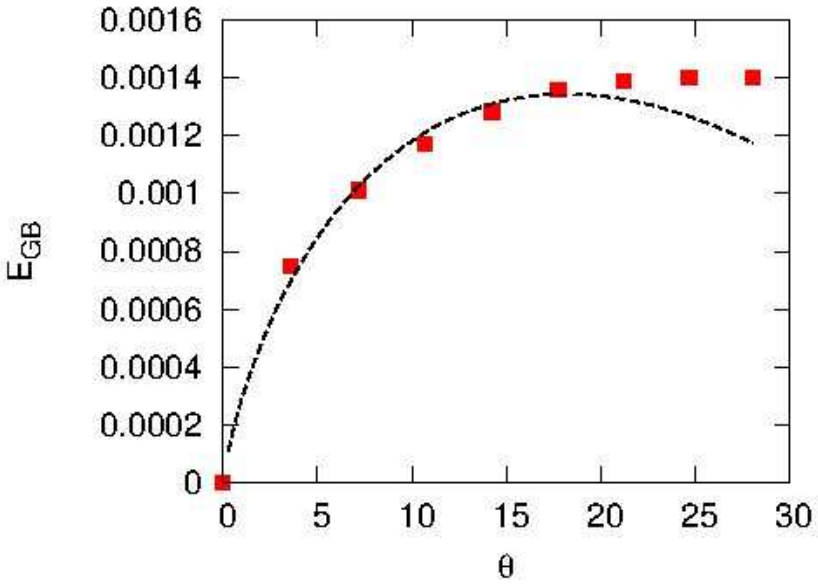

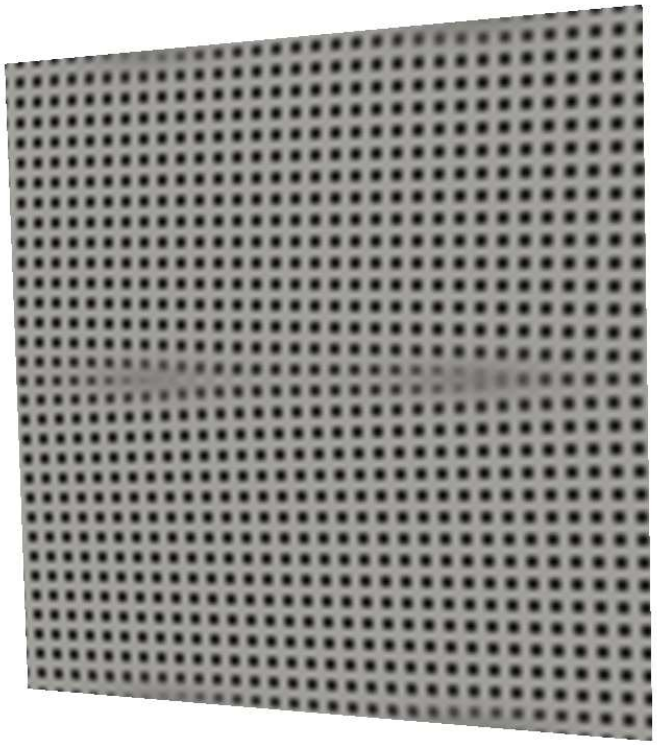

PFC, tilt angle θ = 3.58°

Read and Shockley fit

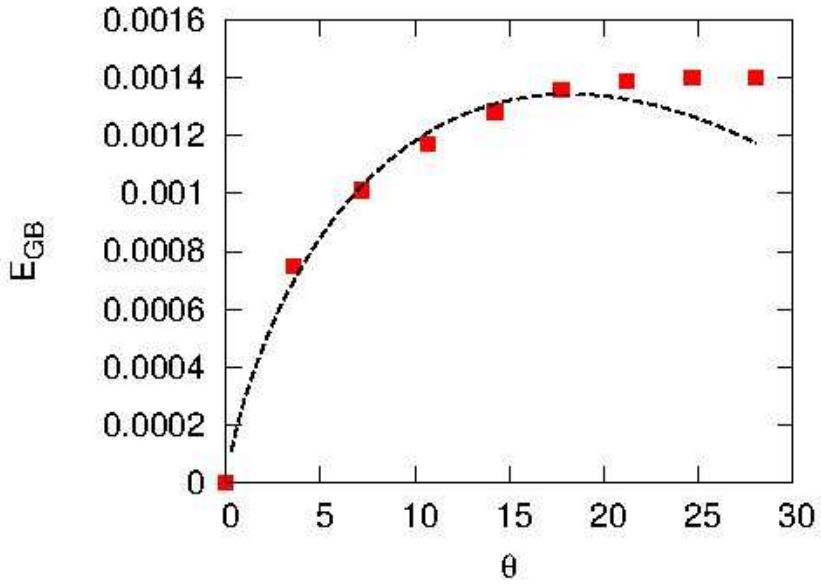

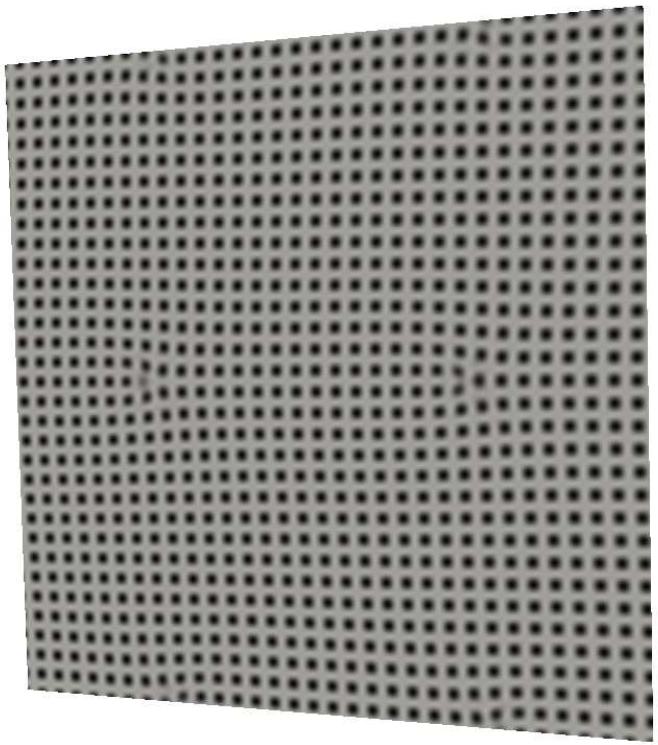

PFC, tilt angle θ = 3.58°

Read and Shockley fit

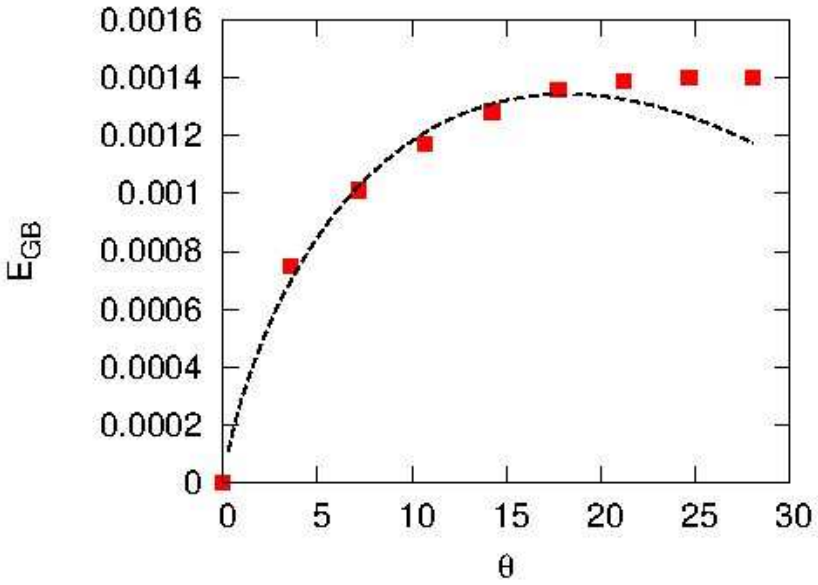

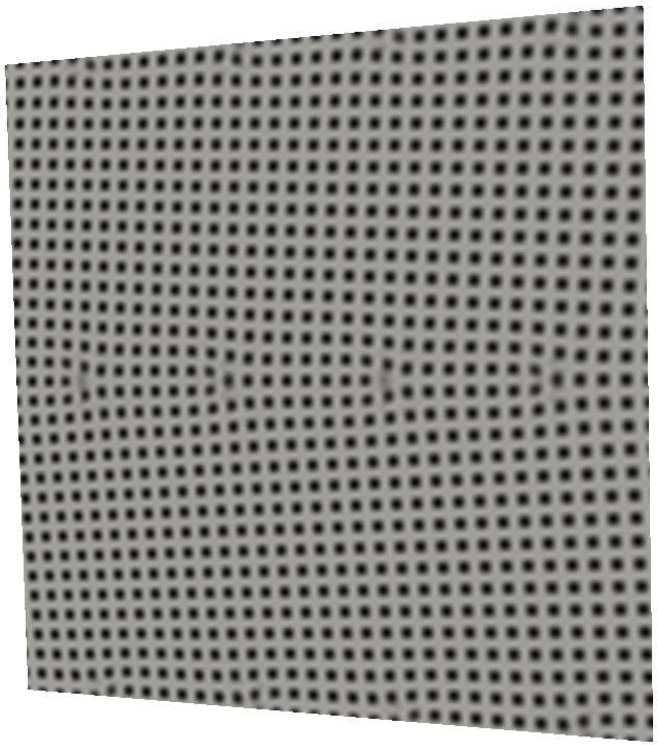

PFC, tilt angle θ = 7.17°

Read and Shockley fit

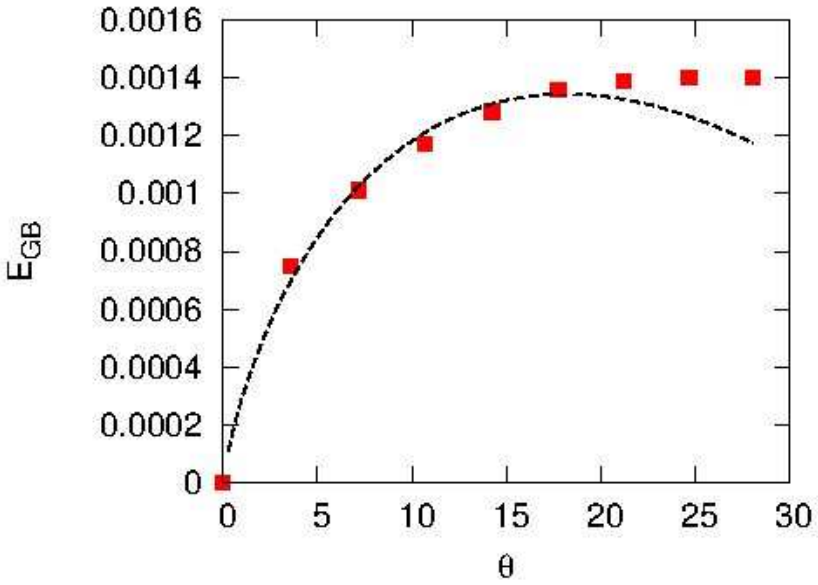

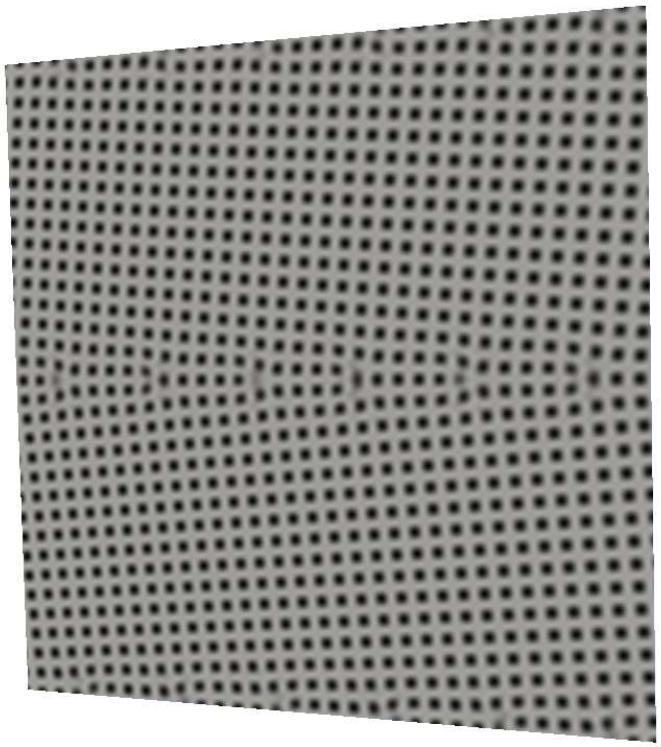

PFC, tilt angle θ = 10.17°

Read and Shockley fit

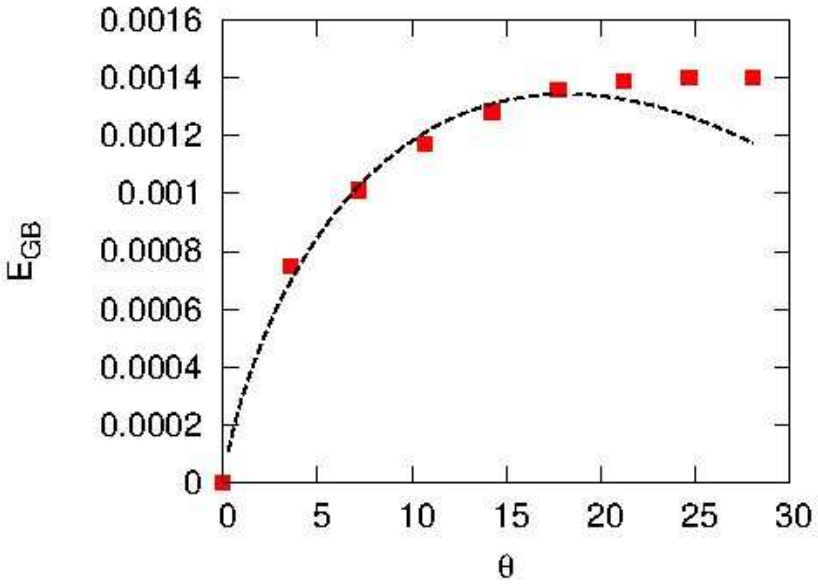

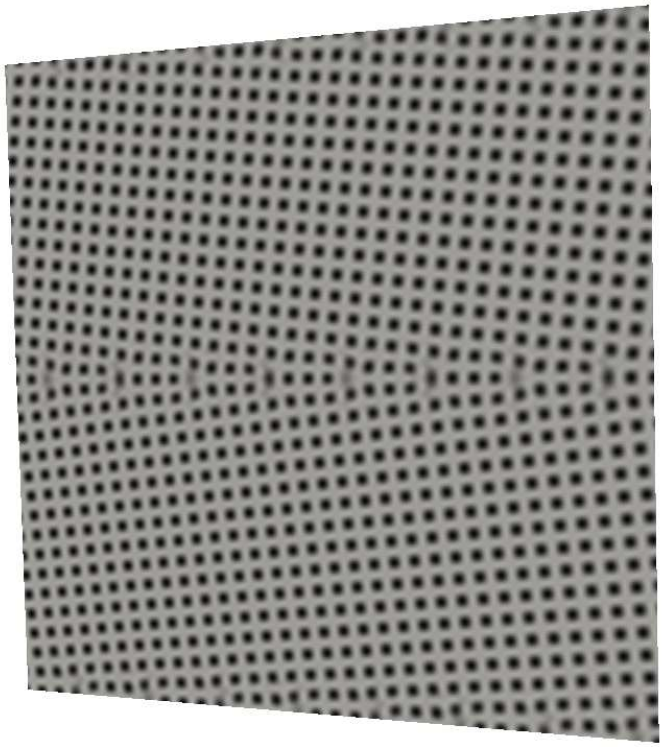

PFC, tilt angle θ = 14.25°

Read and Shockley fit

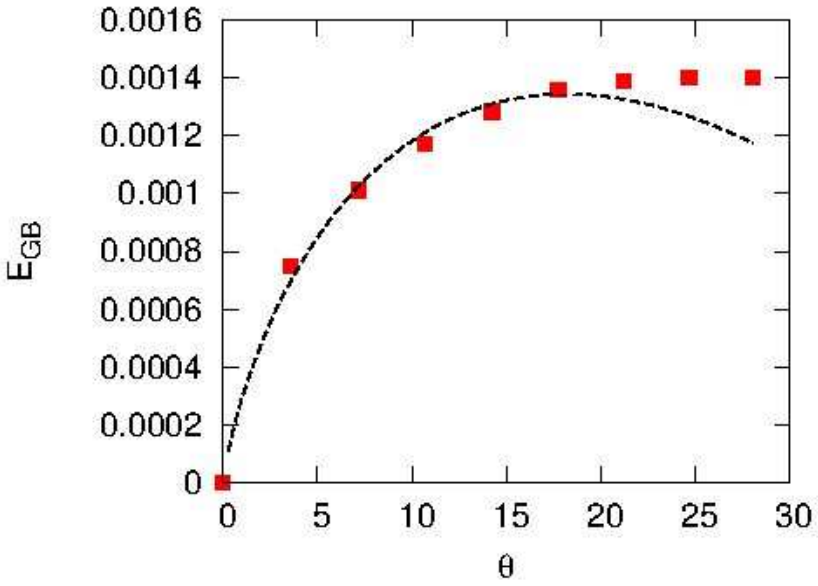

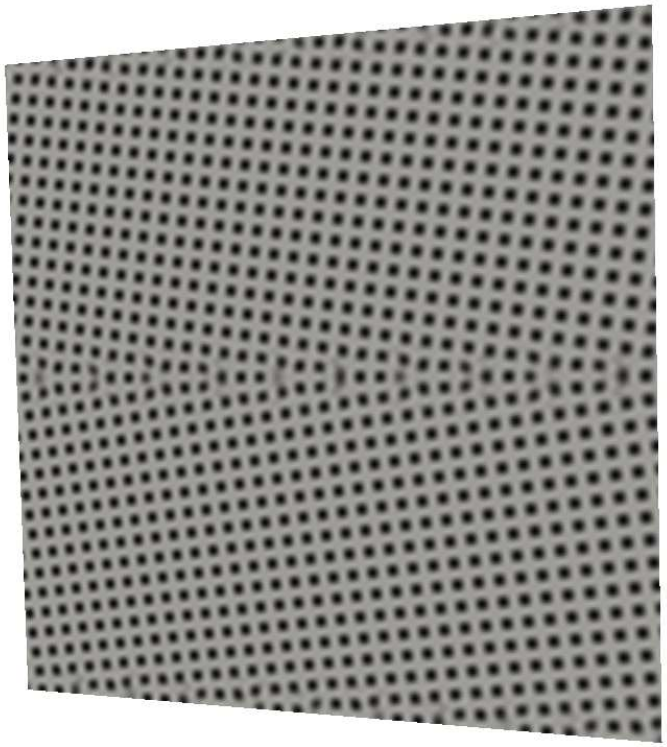

PFC, tilt angle θ = 17.76°

Read and Shockley fit

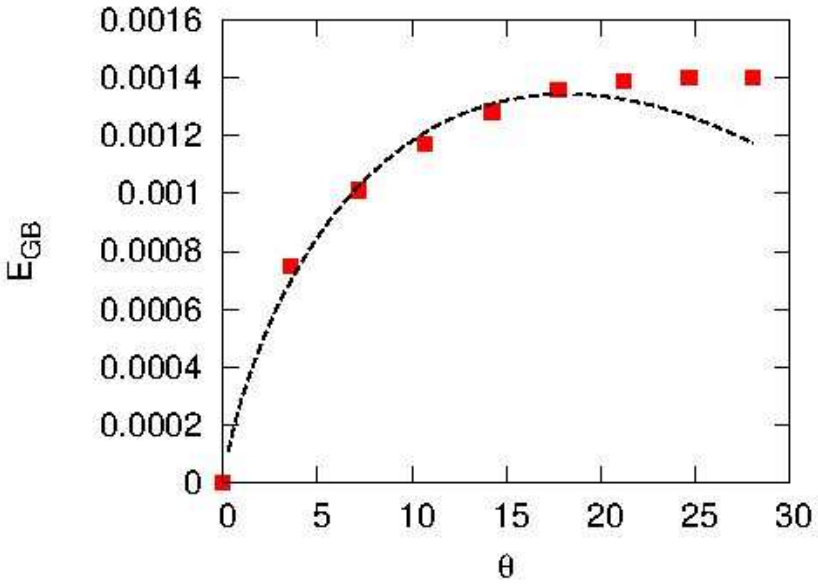

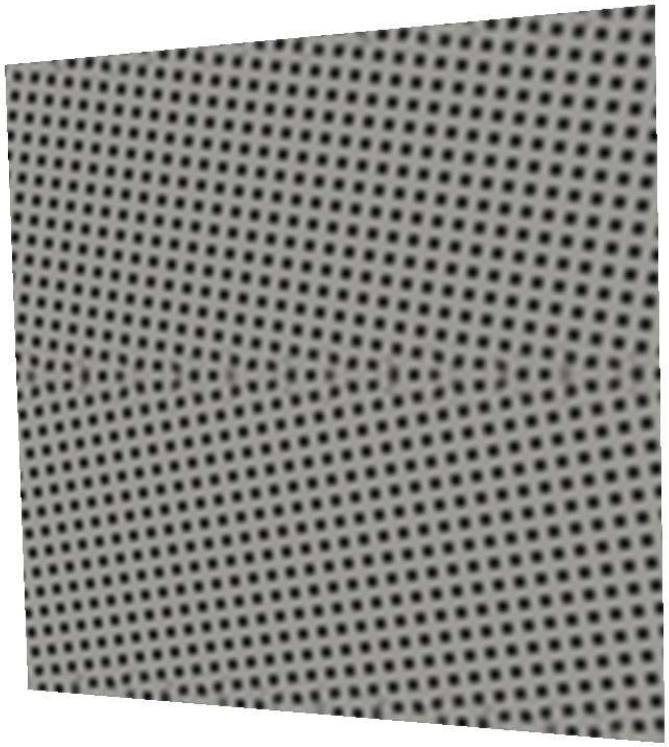

PFC, tilt angle θ = 21.24°

Read and Shockley fit

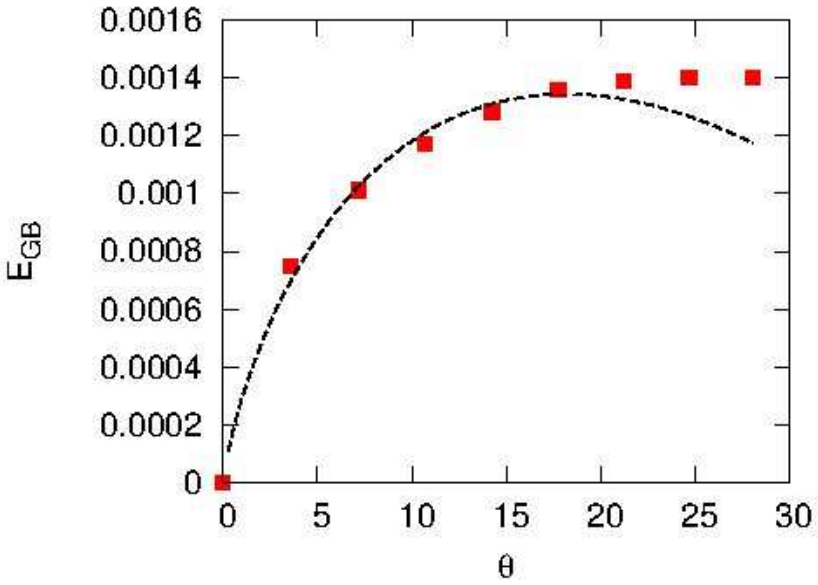

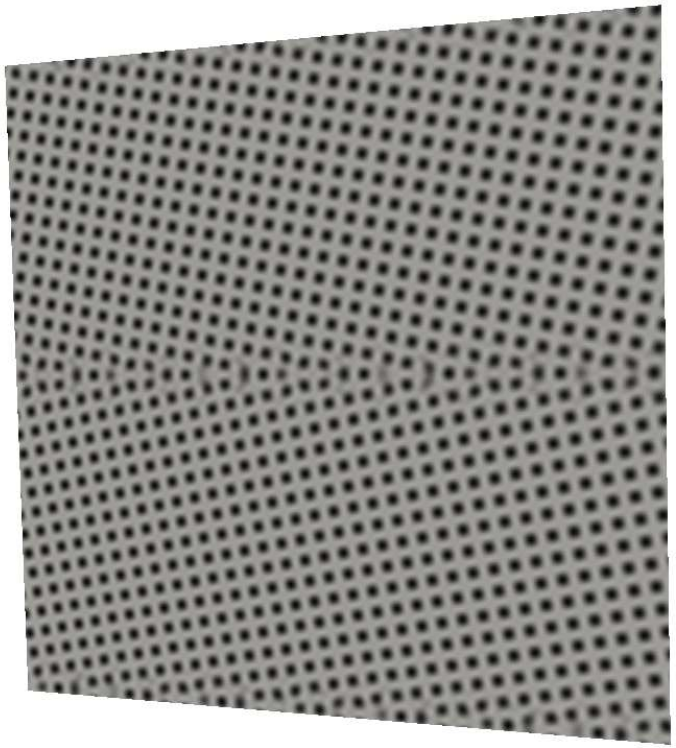

PFC, tilt angle θ = 24.68°

Read and Shockley fit

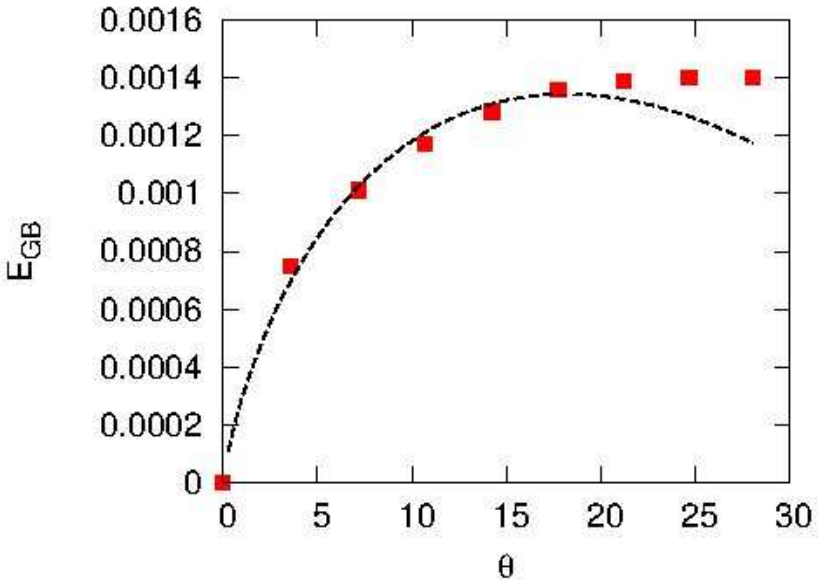

Simulation

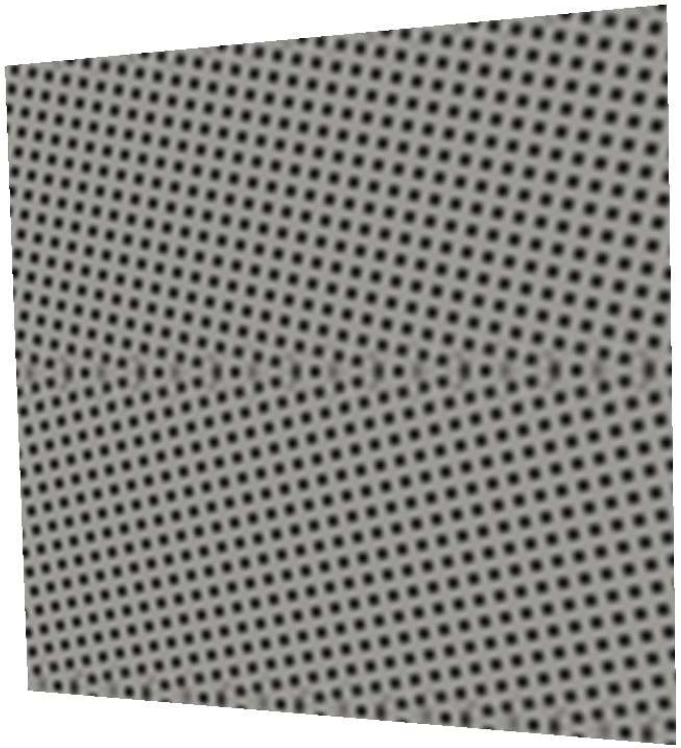

Experimental image

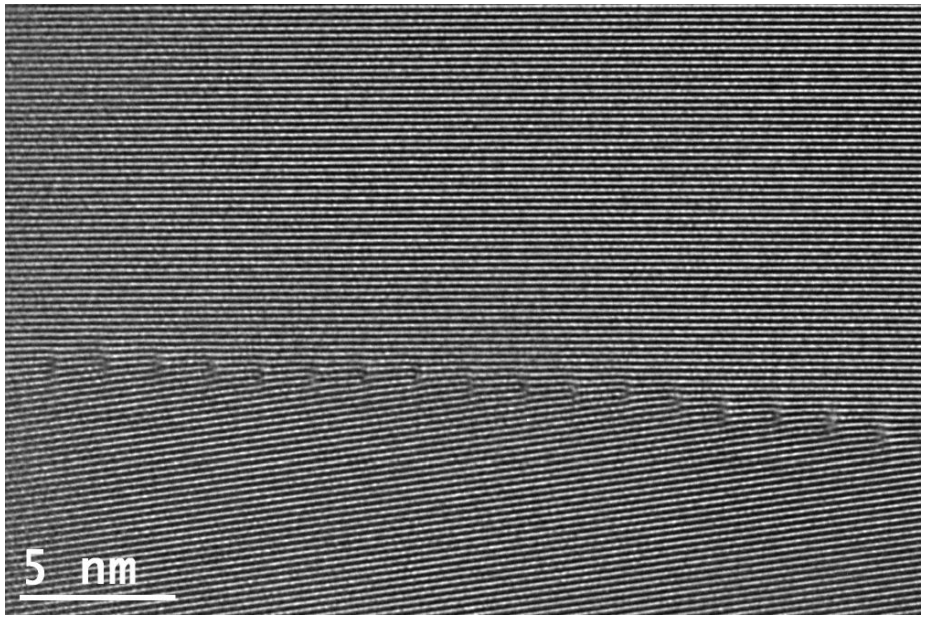

PFC, tilt angle θ = 28.07°

To improve our simulation:

- **More efficient numerical methods to solve TDLG equation**
- **Condition for Δt**

•MD testing of GBs from ADF simulation

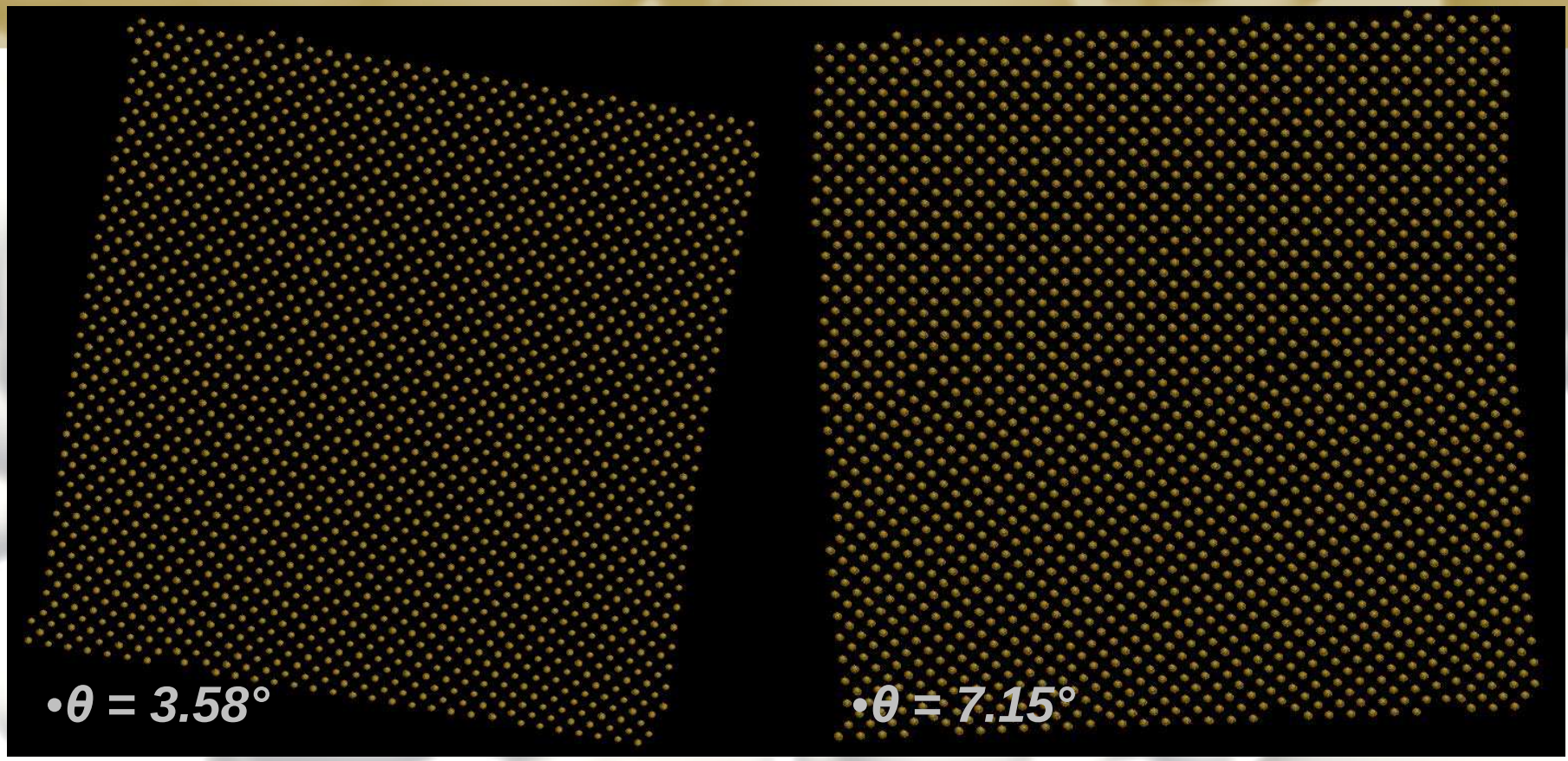

•MD simulation with Ab initio potential for iron,
•realized on the basis of ADF similation results (C. Domain, EDF)

GPM
Groupe de Physique des Matériaux

•GBs in experiment
Qualitative comparison

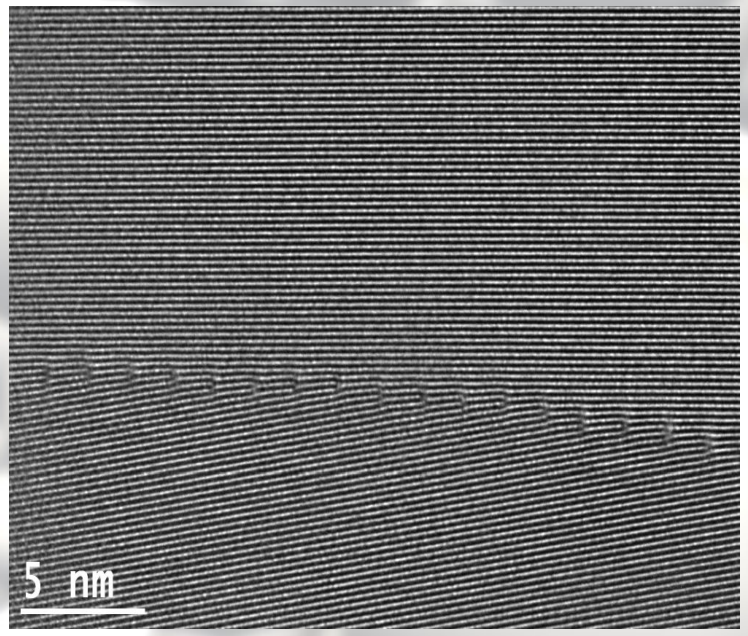

Tilt GB observed in Fe-Al alloy
(X. Sauvage, GPM)

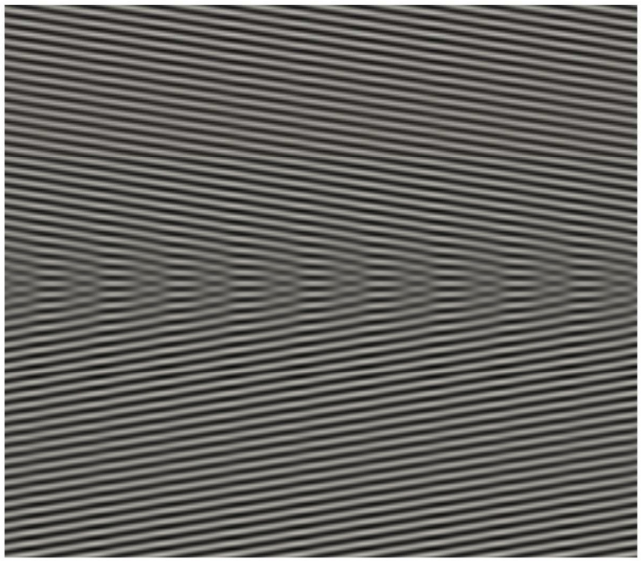

PFC simulations

GPM
Groupe de Physique des Matériaux

•Annihilation of vacancies at GBs in ADF

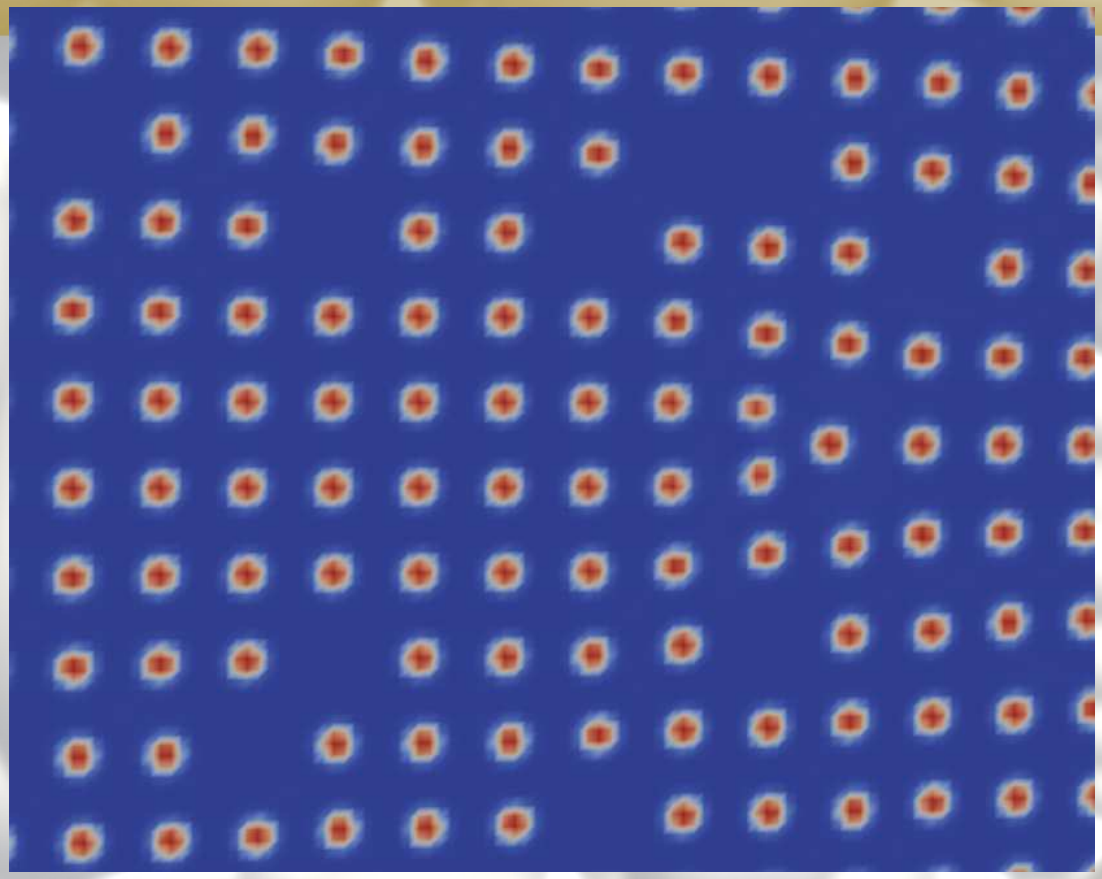

•*t = 0*

•Annihilation of vacancies at GBs in ADF

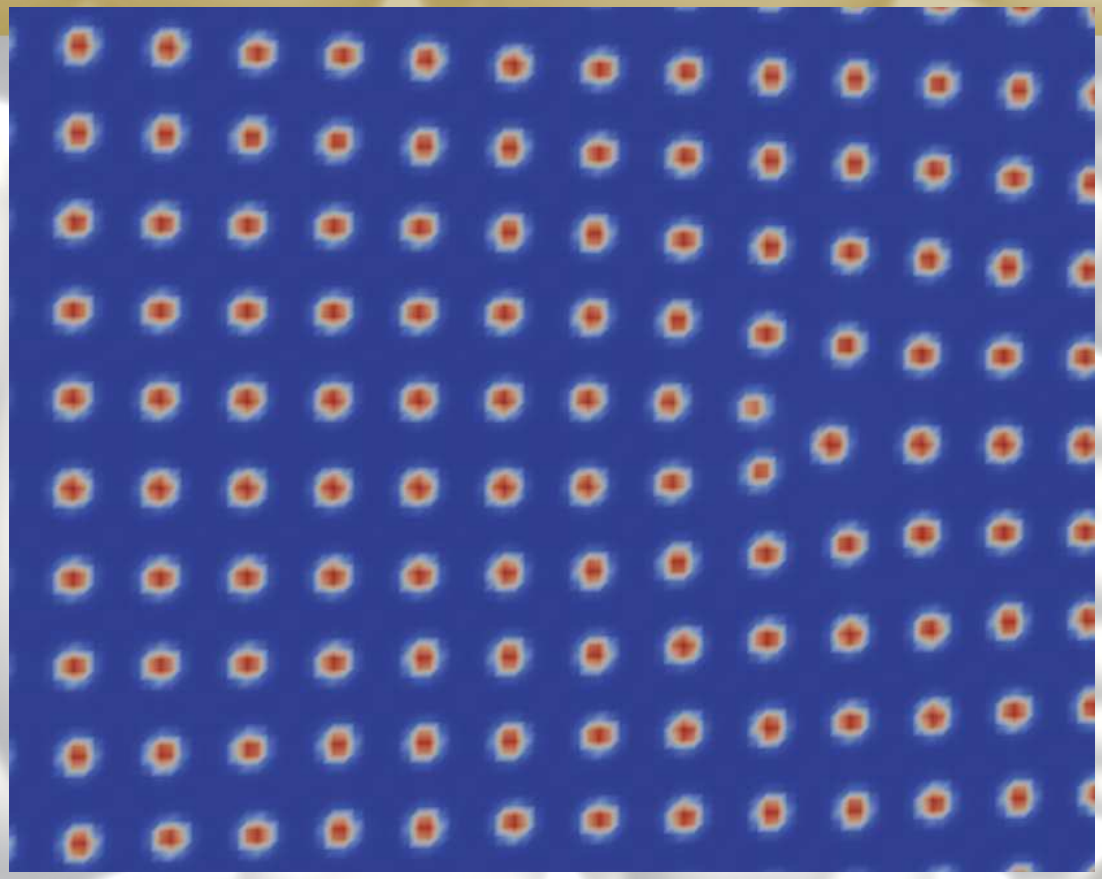

•*t = 50 000*

Groupe de Physique des Matériaux

•Annihilation of vacancies at GBs in ADF

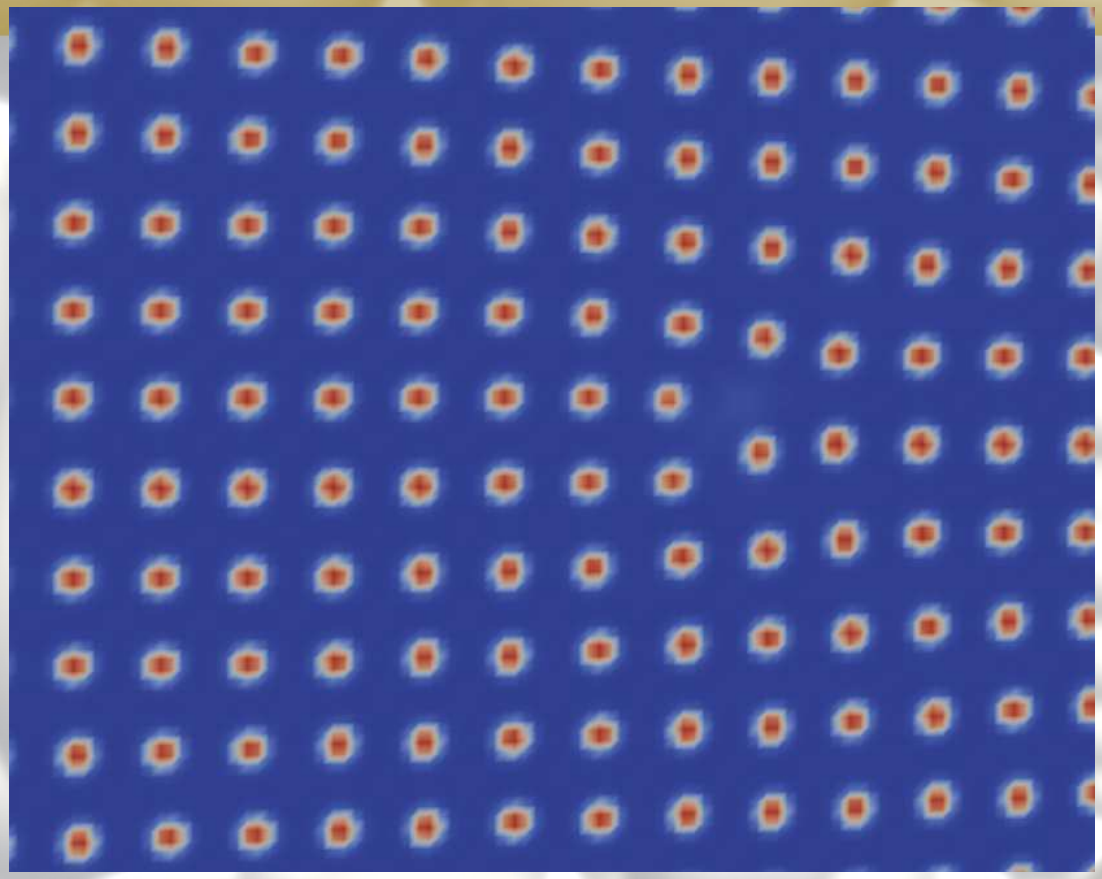

•*t = 200 000*

Groupe de Physique des Matériaux

•Annihilation of vacancies at GBs in ADF

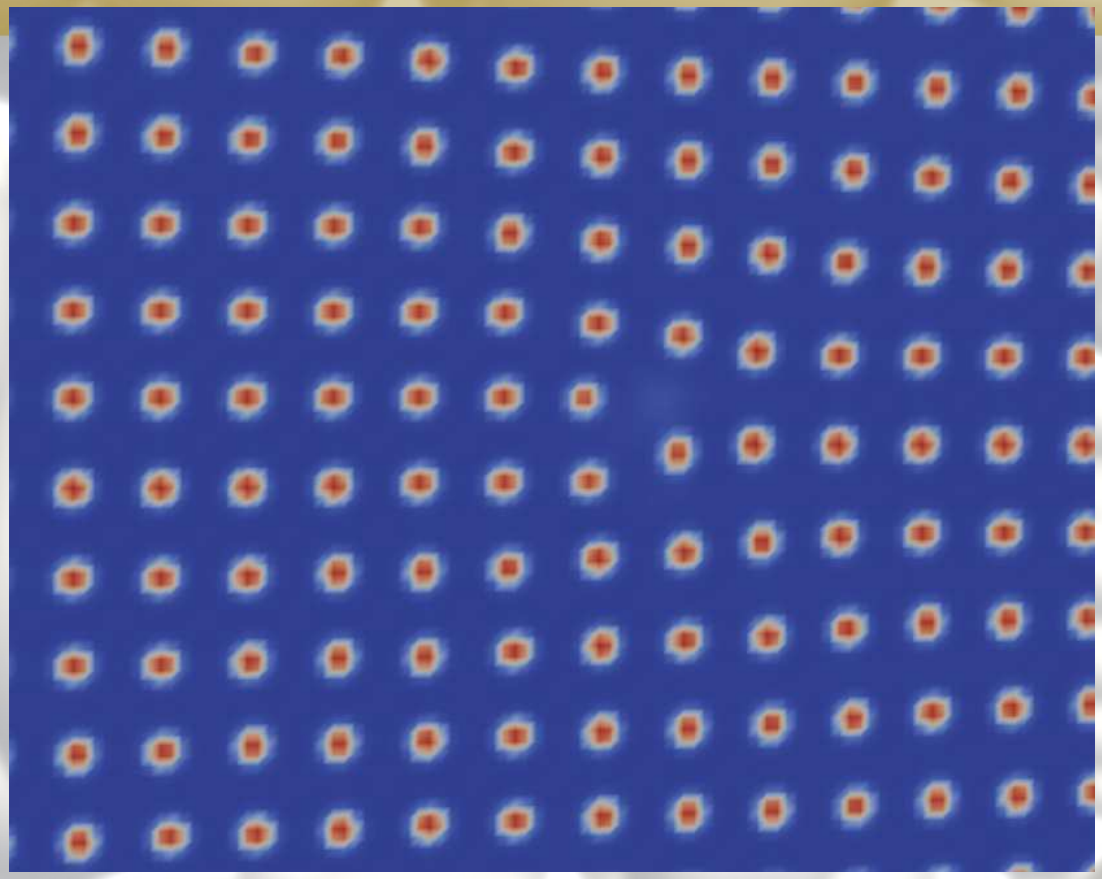

•*t = 400 000*

Groupe de Physique des Matériaux

•Annihilation of vacancies at GBs in ADF

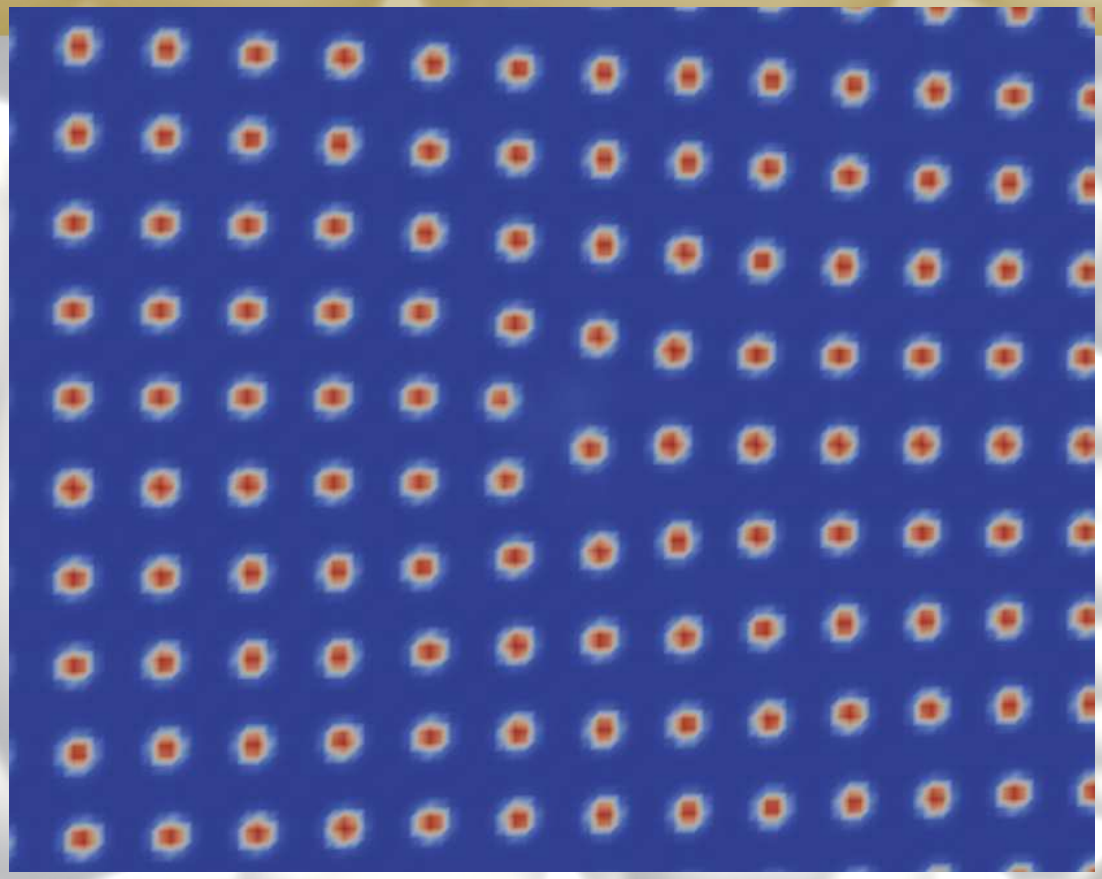

•*t = 700 000*

•Annihilation of vacancies at GBs in ADF

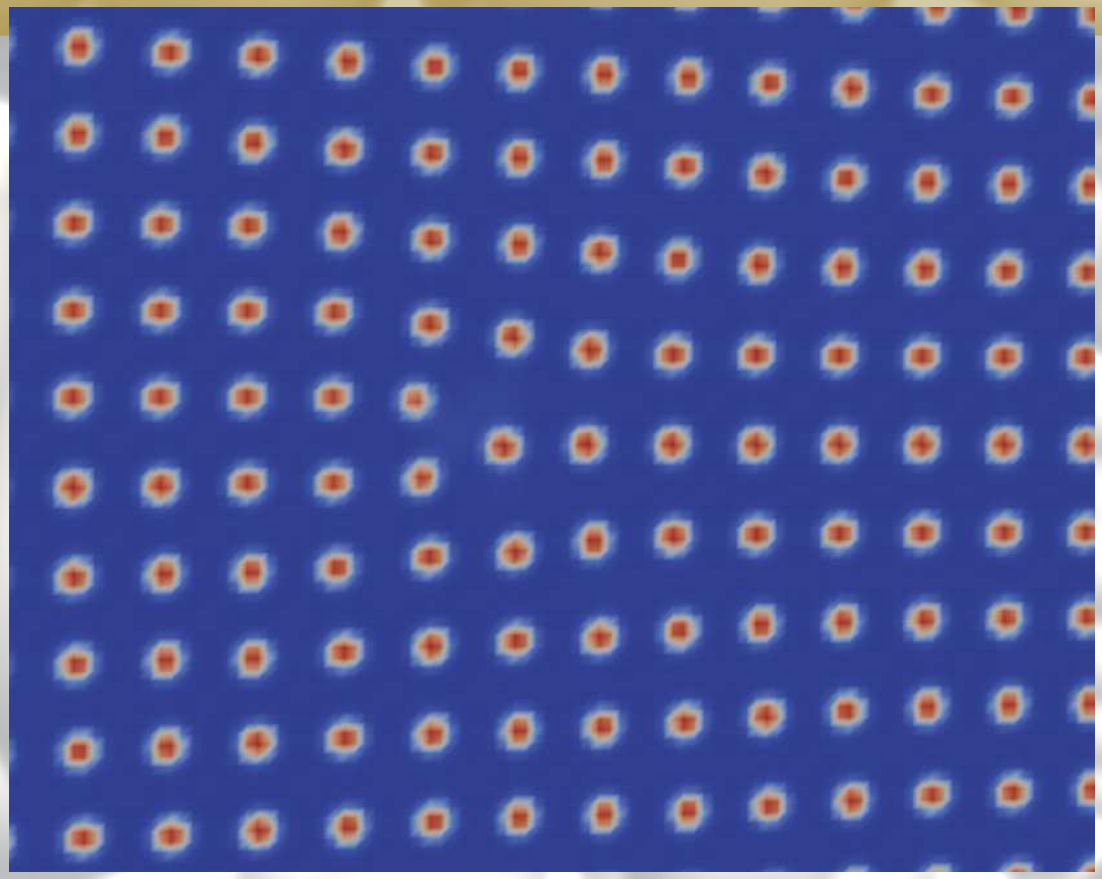

•*t = 1000 000*

Why one minima potential gives only "honeycomb" structure in 2D and bcc in 3D simulations ?

Diffraction pattern of liquid

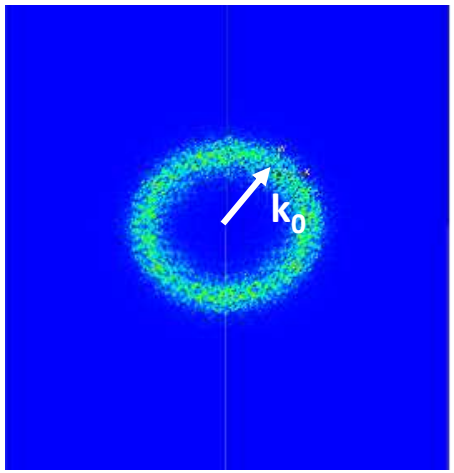

$$I = \rho\left(\vec{k}\right)\rho\left(\vec{k}\right)^*$$

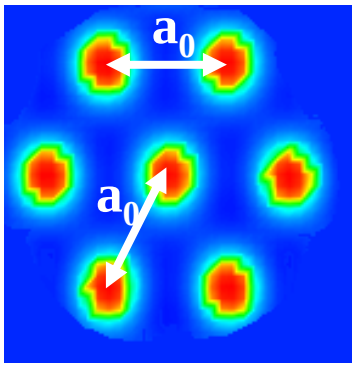

2D structure with one characteristic distance and maximum number of first neighbors.

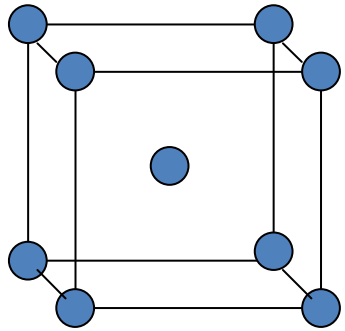

In 3D bcc lattice (fcc reciprocal lattice) the number of first neighbors is maximum

Free energy minima

One mode isotropic potential

The most stable high temperature modification of the crystalline phase is the one whose reciprocal lattice has maximum possible number of the nearest neighbor sites.

FCC to BCC transition
ADF modeling

Initial configuration –> bcc nucleus (r=20 Δ) with KS orientation relation with the fcc parent phase

$$\frac{a_0^{CFC}}{a_0^{CC}} = \sqrt{\frac{3}{2}} \approx 1.225$$

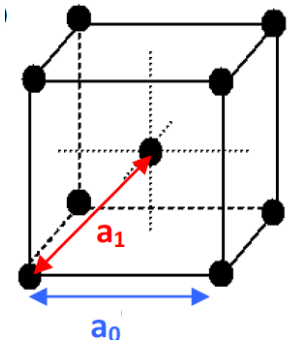

BCC

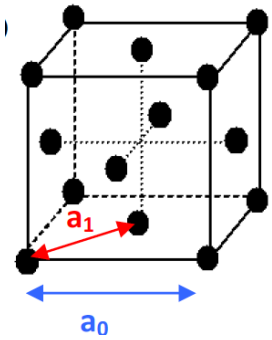

FCC

Simulation box: 256^3

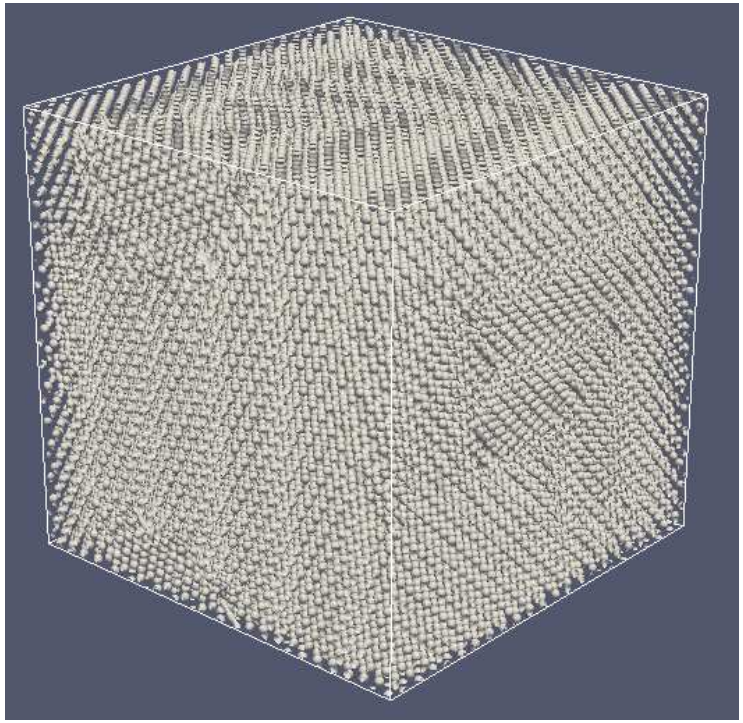

t*=9000

FCC to BCC transition.
ADF modeling

Case II

Bcc embryo r=40 Δ

fcc/bcc K-S relation

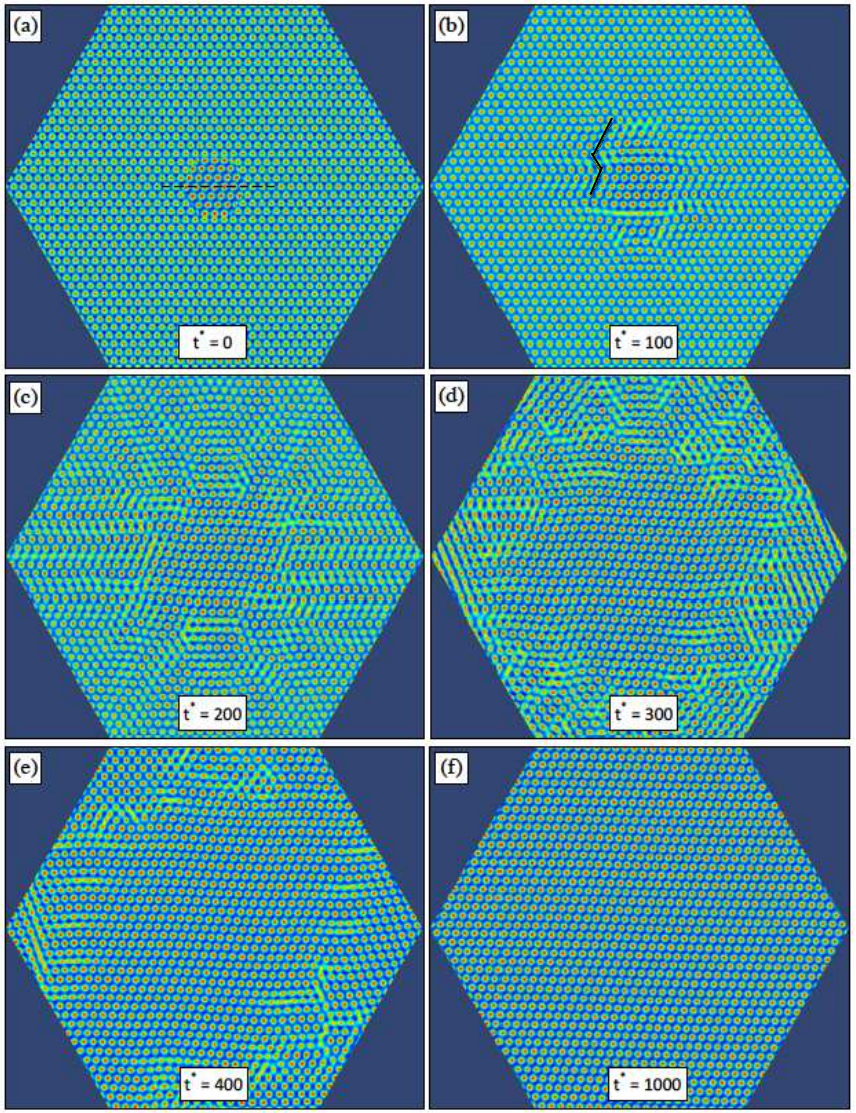

FCC to BCC transition. ADF modeling

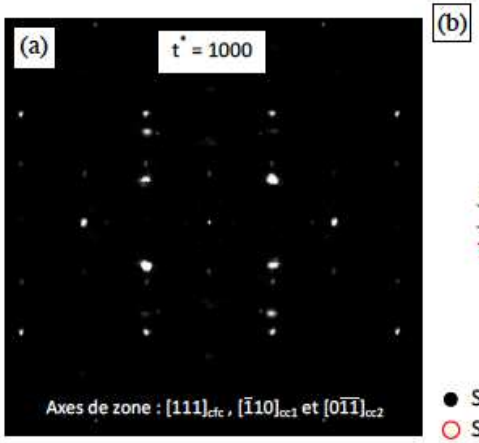

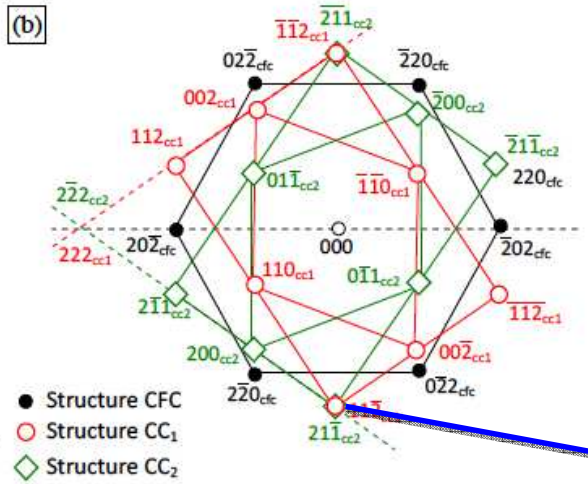

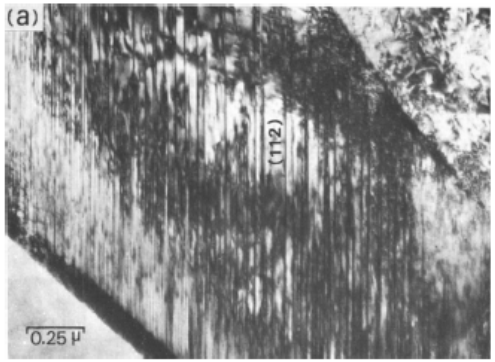

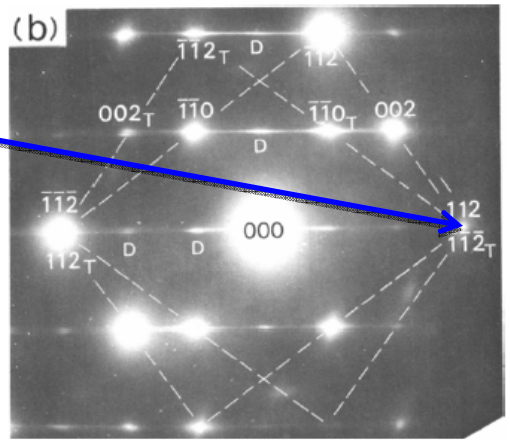

Fig. 7—(*a*) and (*b*). Transmission electron micrograph of {112}$_b$ transformation twins in Kovar (Fe-27.5 pct Ni-17.2 pct Co) martensite and twinned diffraction pattern.

K. SHIMIZU AND Z. NISHIYAMA Met.Mat.Trans. B (1972)

Représentation en trois dimensions des résultats de champ sombre de deux variants de martensite

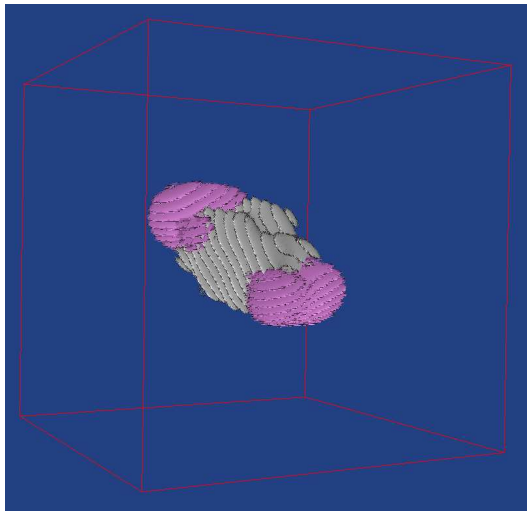

STRIPES ou TUBES (artefact du modèle continue)

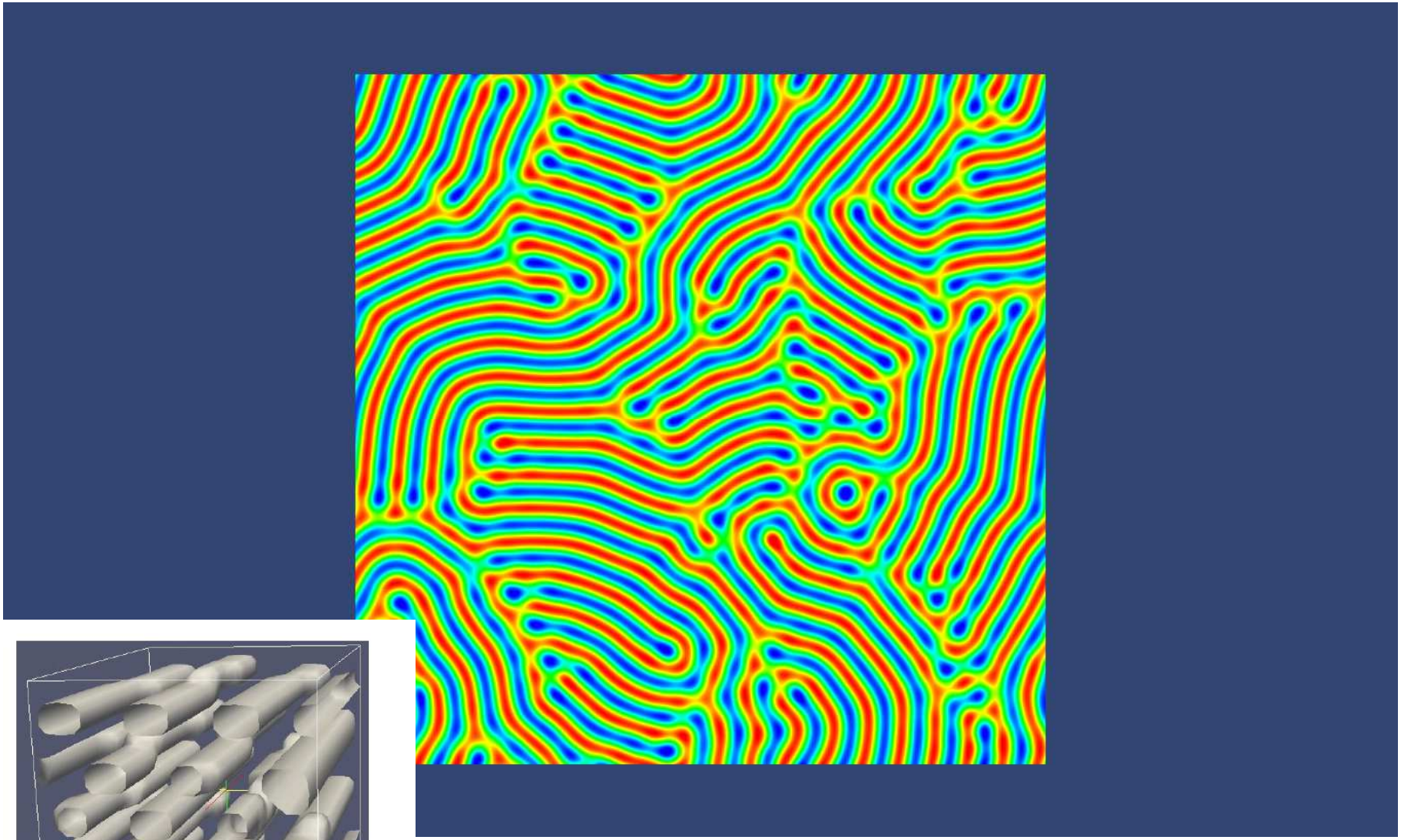

•*PERSPECTIVES*

- **Choice of potentials**
- **Eliminate the artifacts of continuous model.**
- **Model binary alloy and study the segregation of solute atoms at grain boundaries**
- **Carbon atom diffusion in martensite**

GPM
Groupe de Physique des Matériaux